

Durham Research Online

Deposited in DRO:

16 December 2014

Version of attached file:

Accepted Version

Peer-review status of attached file:

Peer-reviewed

Citation for published item:

Saher, M.H. and Gehrels, W.R. and Barlow, N.L.M. and Long, A.J. and Haigh, I.D. and Blaauw, M. (2015) 'Sea-level changes in Iceland and the influence of the North Atlantic Oscillation during the last half millennium.', *Quaternary science reviews.*, 108 . pp. 23-36.

Further information on publisher's website:

<http://dx.doi.org/10.1016/j.quascirev.2014.11.005>

Publisher's copyright statement:

NOTICE: this is the author's version of a work that was accepted for publication in *Quaternary Science Reviews*. Changes resulting from the publishing process, such as peer review, editing, corrections, structural formatting, and other quality control mechanisms may not be reflected in this document. Changes may have been made to this work since it was submitted for publication. A definitive version was subsequently published in *Quaternary Science Reviews*, 108, 15 January 2015, 10.1016/j.quascirev.2014.11.005.

Additional information:

Use policy

The full-text may be used and/or reproduced, and given to third parties in any format or medium, without prior permission or charge, for personal research or study, educational, or not-for-profit purposes provided that:

- a full bibliographic reference is made to the original source
- a [link](#) is made to the metadata record in DRO
- the full-text is not changed in any way

The full-text must not be sold in any format or medium without the formal permission of the copyright holders.

Please consult the [full DRO policy](#) for further details.

1 Sea-level changes in Iceland and the influence of the North Atlantic Oscillation
2 during the last half millennium

3 Margot H. Saher^{1*}, W. Roland Gehrels², Natasha L.M. Barlow³, Antony J. Long³, Ivan D.
4 Haigh⁴ and Maarten Blaauw⁵

5
6 ¹School of Ocean Sciences, Bangor University, Menai Bridge LL59 5AB, UK; ²Environment
7 Department, University of York, Heslington, York YO10 5DD, UK; ³ Department of
8 Geography, Durham University, South Road, Durham DH1 3LE, UK; ⁴Ocean and Earth
9 Science, National Oceanography Centre, University of Southampton, European Way
10 Southampton, SO14 3ZH, UK; ⁵School of Geography, Archaeology and Palaeoecology,
11 Queen's University Belfast, Elmwood Avenue, Belfast BT7 1NN, UK.

12 *Corresponding author (email: m.saher@bangor.ac.uk, tel: 0044 1248 383819, fax: 0044
13 1248 716367)

14
15 **Abstract**

16 We present a new, diatom-based sea-level reconstruction for Iceland spanning the last ~500
17 years, and investigate the possible mechanisms driving the sea-level changes. A sea-level
18 reconstruction from near the Icelandic low pressure system is important as it can improve
19 understanding of ocean-atmosphere forcing on North Atlantic sea-level variability over multi-
20 decadal to centennial timescales. Our reconstruction is from Viðarhólmi salt marsh in
21 Snæfellsnes in western Iceland, a site from where we previously obtained a 2000-yr record
22 based upon less precise sea-level indicators (salt-marsh foraminifera). The 20th century part

of our record is corroborated by tide-gauge data from Reykjavik. Overall, the new reconstruction shows ca. 0.6 m rise of relative sea level during the last four centuries, of which ca. 0.2 m occurred during the 20th century. Low-amplitude and high-frequency sea-level variability is super-imposed on the pre-industrial long-term rising trend of 0.65 m per 1000 years. Most of the relative sea-level rise occurred in three distinct periods: AD 1620-1650, AD 1780-1850 and AD 1950-2000, with maximum rates of $\sim 3 \pm 2$ mm/yr during the latter two of these periods. Maximum rates were achieved at the end of large shifts (from negative to positive) of the winter North Atlantic Oscillation (NAO) Index as reconstructed from proxy data. Instrumental data demonstrate that a strong and sustained positive NAO (a deep Icelandic Low) generates setup on the west coast of Iceland resulting in rising sea levels. There is no strong evidence that the periods of rapid sea-level rise were caused by ocean mass changes, glacial isostatic adjustment or regional steric change. We suggest that wind forcing plays an important role in causing regional-scale coastal sea-level variability in the North Atlantic, not only on (multi-)annual timescales, but also on multi-decadal to centennial timescales.

Key words: diatoms, ocean dynamics, Iceland, Little Ice Age, sea-level rise, NAO

1 Introduction

Determining the nature and causes of sea-level variability in the pre-industrial era provides a long-term context for comparing recent sea-level trends and for developing future projections (e.g. Barlow et al., 2012; Gehrels et al., 2004; Kemp et al., 2011; Milne et al., 2009; van de Plassche, 2000). Driving mechanisms of sea-level changes include mass changes in land-based ice, and other processes such as steric expansion and contraction, and dynamic oceanographic processes including variations in wind stress and atmospheric pressure (Gehrels and Woodworth, 2013).

Unravelling the relative importance of these processes on multi-decadal to centennial timescales requires the development of precise proxy-based sea-level reconstructions that extend before the start of instrumental observations, with good age (decadal) and height (sub-decimetre) control. In the North Atlantic, the most precise reconstructions are developed along low-energy coastlines with small tidal ranges where organic-rich salt marshes provide environments that are suitable for developing continuous sea-level records over the last few millennia (e.g. Gehrels et al., 2005; Kemp et al., 2011).

Identifying the drivers of regional sea-level change demands multiple observations from different parts of any particular ocean basin, which by necessity will be from a variety of depositional and tidal range environments (Long et al., 2014). A variety of microfossil types that include foraminifera, testate amoebae and diatoms are typically used, on their own or occasionally in combination, to constrain palaeomarch surface elevations and past sea-level changes (e.g. Gehrels et al., 2001; Kemp et al., 2009; Charman et al., 2010; Barlow et al., 2013).

In this paper we develop a new relative sea-level (RSL) reconstruction from a meso-tidal salt marsh in western Iceland, an area particularly susceptible to wind-driven sea-level variability

due to its location in the pathway of low pressure systems. In a previous paper Gehrels et al. (2006) reconstructed a 2000-yr record from this site using foraminifera (Fig. 1), and identified a single acceleration in sea level that was dated to the beginning of the nineteenth century. However, the record was heavily dominated by the upper marsh species *Jadammina macrescens* with occasional *Paratrochammina* (*Lepidoparatrochammina*) *haynesi*. This low species diversity provided limited constraints on the elevation of the formation of the past marsh surface, making it impossible to identify any fluctuations in relative sea-level change beyond the 19th century inflection. Here we revisit the study site, Viðarhólmi salt marsh, and focus in on the last five centuries. We exploit the greater sensitivity to elevation (and hence sea level) of diatoms to produce a ~500-yr sea-level reconstruction of high vertical precision. We also apply new chronological analyses to the upper part of the stratigraphic section previously studied to generate an improved age model using new tephra and AMS¹⁴C dates, in combination with previous AMS¹⁴C, ¹³⁷Cs and chemostratigraphical analyses. The resulting reconstruction identifies three distinct periods of rapid sea-level rise during the last ~500 years.

To assess the potential drivers behind these changes we compare the new record to proxy and instrumental reconstructions of the North Atlantic Oscillation (NAO) Index over the same interval. The NAO exerts a strong influence over regional wind patterns, precipitation and temperature, mainly in the winter (e.g. Hurrell et al., 2003). The influence of (winter) NAO (wNAO) on Atlantic sea level during the instrumental era is well established (Andersson, 2002; Haigh et al., 2010; Kolker and Hameed, 2007; Miller and Douglas, 2007; Tsimplis et al., 2005, 2006; Woodworth et al., 2007; Woolf et al., 2003), but its significance in controlling dynamic sea-level variability over longer time intervals has not previously been explored. In this paper we present proxy evidence of at least two pre-industrial oscillations in sea level that broadly correlate to changes in reconstructed wNAO in the North Atlantic

Ocean, highlighting the influence of ocean-atmosphere forcing on regional-scale sea-level variability during past centuries.

2 Study area

Viðarhólmi salt marsh (64.77°N, 22.42°W) is located on the west coast of Iceland (Fig. 1) in an area that has been seismically stable during the late Holocene (Angelier et al., 2004). Árnadóttir et al. (2009) estimate modest rates of uplift due to GIA (~1mm/yr) in the period AD 1993-2004 based on GPS observations, but Gehrels et al. (2006) documented 1.3 m of relative sea-level rise during the last 2000 years, indicating that on millennial time scales this coastal area is subsiding. The marsh is underlain by Tertiary basalt (Ward 1971), and protected by a barrier spit to the south and by an outcropping Holocene lava flow to the east. Several tidal channels dissect the salt marsh. Our fossil sediment section is taken from the cleaned face of one of these channels where a 2 m high peat section is exposed (Figs. 1, 2). This is the same section where monoliths for the Gehrels et al. (2006) study had been taken in 2001 and 2003. Today the salt marsh is largely undisturbed by human influence but is occasionally grazed by sheep. Dominant plants on the marsh are *Carex lyngbyei*, *Agrostis stolonifera*, *Festuca rubra* and *Puccinellia maritima* (Ingólfsson, 1998). Mean tidal range at Viðarhólmi is 2.1 m, mean sea level (MSL) is 0.12 m above the Iceland geodetic datum and the highest astronomical tides reach ~2.1 m above MSL (Gehrels et al., 2006).

Wind patterns in western Iceland are controlled by the position and strength of the Icelandic low pressure system which generally results in dominant wind directions from the east, with only rare westerlies (Einarsson, 1984). During positive phases of the NAO the Icelandic Low tends to deepen and is located further north than during negative phases (Serreze et al., 1997). In the 1930s, for example, the average position of the Icelandic low was at 61°N, while the

shift to a negative NAO mode from the 1940s to the 1970s was associated with a southward movement of this low to around 59°N (Angell and Korshover, 1974). In addition, extra-tropical cyclones tend to track along a more northerly path and are more frequent during a positive NAO mode (Carleton, 1988).

3 Methods

3.1 Field and laboratory methods

In September 2009 we cleaned and re-sampled the upper 60 cm of section 3A of Gehrels et al. (2006) using monolith tins driven into the cleaned sediment surface. The lithostratigraphy of the marsh is detailed in Gehrels et al. (2006) and mainly comprises sandy peat (Fig. 2). Sand- and silt-sized material in the section is of volcanic origin and includes tephra. Three distinct horizons of silt are visible in the sequence at 54 cm, 34 cm and 14 cm. Section 3A contains an orange-brown pumice at 58-60 cm, dated to 1226/7 (Gehrels et al., 2006), which we used as the base of the re-sampled section.

We sampled modern diatoms from four transects across a height range of 0.74 m (35% of the tidal range) from just above the Highest Astronomical Tide (HAT) to the coring site in the lower part of the mid marsh at an elevation between Mean High Water Springs (MHWS) and Mean High Water (MHW) (Fig. 1, Supplementary information Table 1). Surface samples were collected with a cylindrical turf cutter. The top 1 cm was sub-sampled in the laboratory for diatom analysis. Heights of sample sites were surveyed relative to geodetic and tidal datums with a Total Station. Samples for diatom analysis were prepared using the techniques detailed in Palmer and Abott (1986). Diatoms were identified using Foged (1974), Hartley et al. (1996), Hemphill-Haley (1993), van der Werff and Huls (1957-1974) and classified by the halobian classification system (Hustedt, 1953, Hemphill-Haley, 1993).

3.2 Transfer functions

We applied a transfer function (Birks et al., 1990) based on present-day microfossil assemblages to obtain estimates of palaeomarch surface elevation from the down-core fossil assemblages. Using detrended canonical correspondence analysis (DCCA) in CANOCO version 4.5 (ter Braak and Smilauer, 2002) we calculated the length of the environmental gradient of the modern diatom dataset at 2.2 standard deviation units. We therefore followed the general rule of thumb that, because the DCCA gradient length is greater than 2 standard deviation units, sufficient species in the training set have their optima located along the environmental gradient and are collectively responding unimodally to elevation across the marsh surface (ter Braak and Prentice, 1988). We developed a unimodal weighted averaging partial least squared (WA-PLS) model (ter Braak and Juggins, 1993) using the software C² (Juggins, 2003). We selected a WA-PLS model with two components ($r^2 = 0.75$, Root Mean Squared Error of Prediction (RMSEP) = 0.09) as this provided a >10% improvement in r^2_{boot} and RMSEP compared to a one component model. Adding further components did not significantly improve model performance. The observed *versus* predicted marsh surface elevations are shown in Fig. 3. The WA-PLS diatom model predicts the elevation of the core top to within 1 cm.

We evaluated the similarity between the modern and fossil assemblages, and therefore the robustness of our reconstructions, using the modern analogue technique (MAT) (Overpeck et al., 1985; Jackson and Williams, 2004). We considered fossil samples with a minimum dissimilarity coefficient (minDC) smaller than the 5th percentile as having a good analogue, those with a minDC between the 5th and the 20th percentile as having a close analogue, and those with a minDC of more than the 20th percentiles as having a poor modern analogue (Simpson, 2007, Watcham et al., 2013). We removed all samples with a poor modern analogue from our resulting RSL reconstructions.

3.3 Chronology

We added nine high-precision AMS¹⁴C dates (Bronk Ramsey et al., 2007), four bomb-spike AMS¹⁴C dates, and a tephra marker to the existing chronological data of Gehrels et al. (2006) (Table 1). The chronology of the 2006 record was based on conventional AMS ¹⁴C, ¹³⁷Cs, Pb/Li, ²⁰⁶Pb/²⁰⁷Pb and magnetic declination measurements. The new high-precision AMS ¹⁴C dates were obtained from fragile, horizontally embedded, detrital plant remains, and the exoskeletons of a (non-burrowing) weevil (*Otiorhynchus* sp.). These analyses were conducted at the NERC Radiocarbon Facility within the Scottish Universities Environmental Research Centre, East Kilbride, Scotland.

Within the core we detected tephra that erupted in AD 1721 from the Katla volcano located ca. 200 km southeast of Viðarhólmi. This is an exceptional find because other historic Katla tephras (such as AD 1755) were transported by winds in a northeasterly direction and did not reach our field site (Haflidason et al., 2000). The original Gehrels et al. (2006) age model suggested that the Katla AD 1721 tephra (Larsen, 2000) could be located in the sampled sequence between 34 and 48 cm. We therefore targeted this depth range at 1 cm intervals, sieving samples and examining the 25-63 µm fraction under a light microscope. About 60 tephra shards were picked from each sample, and prepared for electron probe analysis at the School of Geosciences, University of Edinburgh. We selected 154 grains on the basis of successful preparation and pristineness of the material, and analysed their chemical composition on a Cameca SX100 electron microprobe, with rhyolitic (Lipari) and basaltic (BCR2g) standards used for calibration (see Hayward, 2012). We identified 39 grains with Katla geochemistry (Einarsson et al., 1980; Óladóttir et al., 2008) (Supplementary Information Table 2), of which nine had the characteristic K₂O/P₂O₅ signature of historic Katla eruptions (Óladóttir et al., 2008). A maximum of five historic Katla grains per sample were found at 39 cm; all other samples contained one shard at most. On this basis we

assigned a date of AD 1721 to the level at 39 cm, assuming that bioturbation and remobilisation by wind and water subsequently re-distributed some shards over a wider depth range (e.g. Davies et al., 2007; Gehrels et al., 2008).

We developed our age-depth model (Fig. 3) using the Bacon package in R (Blaauw and Christen, 2011). Bacon requires as input a prior mean accumulation rate which we calculated using the depth of the AD 1226-7 pumice tephra at 58 cm (Gehrels et al., 2006; Haflidason et al., 1992; Sigurgeirsson 1992). In the 2001, 2003 and 2009 monoliths the pumice tephra was found at 58 cm, suggesting negligible sedimentation between sample collection dates. Although this does not allow us to reconstruct sea-level changes during the past decade, it does enable all analyses to be easily combined into one chronology. The stratigraphy and our age-depth model do not show evidence of other significant hiatuses in the record.

3.4 Sea-level reconstructions

We translated the palaeo-marsh elevations calculated by the transfer functions into relative sea level (RSL) using the equation:

$$\text{RSL (m)} = \text{sample height (m MSL)} - \text{palaeo-marsh elevation (m MSL)} \text{ (e.g. Gehrels, 1999)}$$

Results are presented in Table 2. The sample-specific bootstrapped RMSEP gives the vertical uncertainty (approximate to 1σ) for each fossil sample, although in the figures we multiplied the errors by 1.96 to 2σ . All sample ages and errors are based on modelled ages; those from dated levels have reduced uncertainties compared to those from intermediate (undated) levels. On the basis of four ^{14}C -dated sea-level index points that directly overlie bedrock, Gehrels et al. (2006) concluded that the section is free of any significant compaction. This is in agreement with the compaction studies of Brain et al. (2012) who found that thin,

lithologically homogeneous stratigraphies, like the one described here, are not significantly affected by compaction.

To calculate error envelopes for our sea-level reconstruction we resampled the RSL data points in R using their individual age and vertical error estimates. For each of 1,000 iterations, we sampled random values from the means and (1 standard deviation) errors of the age and RSL estimates (assuming normal distributions) and calculated smooth splines (smoothing parameter 0.8) through the resampled data points. From the resulting family of 1,000 smooth splines, we calculated 68% confidence ranges every 5th year between AD 1500 and 2000. We determined the corresponding rises based on the derivatives of the above smooth splines.

4 Results

4.1 Modern diatoms

The modern diatom flora of Viðarhólmi salt marsh is diverse, but the 28 taxa with an abundance of >5% of the total diatom valves counted (TDV) exhibit a strong vertical zonation across the marsh (Fig. 5). Assemblages are dominated by the genus *Navicula*, with as most abundant species *N. ignota*, *N. cincta* type, and *N. salinarum*. Other abundant species are *Luticola mutica* and *Nitzschia filiformis*.

4.2 Fossil diatoms

Fossil diatoms (Fig. 6) in the lower part of the core (~45-55 cm) are characterised by relatively high percentages (up to 40% TDV) of freshwater species such as *Pinnularia borealis*. From ~45 cm upward, the fresh- to brackish-water taxon *Navicula cincta* type dominates, with a maximum abundance of 71% TDV at 27 cm. In the upper 10 cm, *Luticola mutica* increases in abundance (max. 34% TDV).

4.3 Age-depth model

The age model shows a gradual increase in sedimentation rate from ~0.2 mm/yr at the base of the sequence to 3 mm/yr near the top (Fig. 4). The sample-specific age uncertainties vary through the section: 95% uncertainty intervals are ~40 years between AD 1570-1650, ~20-30 years between AD 1775-1895 and ~10-20 years in the periods AD 1650-1775 and AD 1895-1950. Age uncertainties are smallest (<10 years) from AD 1950 onwards. Age uncertainties of our sea-level reconstruction are smaller than those of the individual data points (Fig. 3) due to the Bayesian nature of the calculation. The Bayesian algorithms prohibit age-models with reversals, so that ages that are highly anomalous do not feature strongly in the final age model.

4.4 Quantitative relative sea-level reconstructions

We combine the reconstructed marsh surface elevations (Fig. 6) with the age-depth model (Fig. 4) to produce a new record of past RSL change (Fig. 7A). Figure 7B shows the amended sea-level reconstruction for the past 2000 years, including the older data points of Gehrels et al. (2006). The diatom-based transfer function predicts a palaeommarsh surface elevation for the new samples with close/good modern analogues of 1.84 to 2.03 m. This falls within the range of the palaeommarsh surface elevations independently estimated by the foraminifera results in Gehrels et al. (2006). The elevation estimates are primarily controlled by species *Navicula ignota*, *Fragilariforma virescens* and *Opephora marina*. Overall, the reconstruction shows a RSL rise of ~0.6 m in the last 500 years. Most of the sea-level rise appears to have occurred in three steps, with rapid rise in the 17th century, the late 18th to early 19th century and the 20th century.

5 Discussion

5.1 Comparison with other records

The diatom-based transfer function produces a robust reconstruction that lies within the error bars of, and thus is corroborated by, the original foraminifera-based reconstruction from this site (Gehrels et al., 2006; Fig. 1C). The high species diversity and species turnover of the diatoms, similar to those found by Patterson et al. (2000) in British Columbia, Canada, reveal several decadal-scale fluctuations in sea level not resolved in the original foraminifera-based reconstruction. Despite samples with poor modern analogues, especially towards the base and in the uppermost samples, we can resolve several sea-level fluctuations.

The pronounced RSL inflection at ~AD 1820 in the foraminifera-based reconstruction for Viðarhólmi salt marsh (Gehrels et al., 2006) was largely due to an abrupt change in the original age-depth model. Our new age model is smoother and as a result the rapid acceleration is removed. The latter part of the record shows a good fit with the Reykjavik tide-gauge record (Fig. 7A).

The overall rise in RSL identified in our new reconstruction (Fig. 7A) of 0.6 m during the last ~500 years cannot be directly compared with global sea-level reconstructions, such as that of Jevrejeva et al. (2006), as the latter is corrected for glacial isostatic adjustment (GIA). We do not correct our record for GIA, as the best available data based on Global Positioning System (GPS) data amounts to ~1 mm/yr uplift (Árnadóttir et al., 2009), which is not compatible with the millennial-scale relative sea-level rise documented in the Viðarhólmi sediments (Gehrels et al., 2006). We therefore instead focus on fluctuations in the sea-level record which may provide clues for driving mechanisms.

Interestingly, the proxy RSL reconstructions from the eastern USA (Kemp et al., 2011, 2013), Nova Scotia (Gehrels et al., 2005) and north-west Scotland (Barlow et al., 2014) show little variability during the past millennium before a late 19th to early 20th century inflection. These differences between the Icelandic and other North Atlantic records suggest that regional/local influences play a significant role in driving sea-level variability.

5.2 West Icelandic sea level and NAO

The multi-decadal variability observed in our new Iceland record is reminiscent of the fluctuations observed in the North Atlantic Oscillation (NAO) (e.g. Cornes et al., 2013; Hurrell and van Loon, 1997; Jones et al., 1997; and Luterbacher et al., 1999). We therefore first explore the relationship between the NAO and sea level in instrumental records, and then test the hypothesis that the periods of rapid sea-level rise in our Icelandic salt-marsh proxy record are synchronous with reconstructed changes in NAO.

The influence of the NAO on sea level has been established in different areas such as the North Sea area (Wakelin et al., 2003) and the Baltic (Andersson, 2002). The NAO, which is defined as the pressure difference between the Azores High and the Icelandic Low, can affect Icelandic sea level through air pressure changes and wind stress. Air pressure will influence sea level in its vicinity due to the inverted barometer effect which is ~1cm/mbar (Ponte, 1992; Wunsch and Stammer, 1997); as air pressure rises (falls) so sea level falls (rises). The annual average pressure recorded by the Stykkishólmur weather station (~40 km from our field site; see Fig. 1) has varied by 12 mbar over the observational period (AD 1949-2012), which would translate into sea-level fluctuations of ~12 cm. The NAO, however, is mainly a winter phenomenon, and intra-annual variations in average winter (DJF) air pressure are considerably larger at 26 mbar. Additionally, the Icelandic Low dominates the wind patterns

in the vicinity of our field site, and this pressure system is also known to influence sea level (e.g. Douglas, 2008; Hong et al., 2000; Kolker and Hameed 2007).

To evaluate the possible effect of NAO on west Icelandic sea level, we compare (Fig. 8A-D) annual mean relative monthly sea level (RMSL) records from Reykjavik, with time-series of air pressure, wind speed, and wind direction, averaged across a box encompassing our study area (see Fig 9), and the NAO index (<http://www.cru.uea.ac.uk/~timo/datapages/naoi.htm>).

The time-series of air pressure, wind speed and wind direction were derived from MSL pressure and 10 m wind fields, obtained from the 20th century global reanalysis dataset (Compo et al 2011). These meteorological fields are available at a resolution of a data point every 6 hours from 1871 to 2011 and have a horizontal resolution of 2°. Data were downloaded from the reanalysis web page (http://www.esrl.noaa.gov/psd/data/20thC_Rean/).

We generated both annual averages and winter (DJF) averages (Fig. 8A-D). To reduce the considerable year-to-year variability we applied a 9-year running average (Fig. 8E-H) to the derived time-series (which is similar to the resolution of our proxy sea-level record). As expected, there is a negative correlation between (9-year smoothed) air pressure and MSL (annual: $r^2=0.08$; winter: $r^2=0.27$), which is explained by the inverted barometer effect. There is a positive correlation between MSL (9-year smoothed) and wind direction (annual: $r^2=0.01$; winter: $r^2=0.26$). There is a stronger (positive) correlation between MSL (9-year smoothed) and the NAO (annual: $r^2=0.27$; winter: $r^2=0.53$); and wind speed (annual: $r^2=0.54$; winter: $r^2=0.41$).

To further compare the atmospheric circulation near Iceland with the Reykjavik tide-gauge record, we detrend the tide-gauge record (using a linear trend fitted to the complete MSL time-series) to remove lower-frequency variability such as that associated with changes in ocean volume. We subdivide the tide-gauge data into years in which MSL was $>+1$ sd,

324 0<+1sd, 0>-1sd, and <-1sd, and calculate the average atmospheric patterns, over the period
325 AD 1871-2011, for these categories (Fig 9).

326 As noted above; the Icelandic Low, a persistent centre of low atmospheric pressure off the
327 west coast of Iceland, tends to be deeper when sea levels at Reykjavik are higher. The
328 dominant wind pattern involves strong winds from both the north and the south, resulting in a
329 weak (though still significant) correlation of wind direction with MSL, and a strong
330 correlation with wind strength. The combined wind domains generate set-up on the western
331 Icelandic coast.

332 The instrumental data reveal a strong correlation of NAO-related factors with instrumental
333 measurements of sea level. In order to evaluate a potential link between our ~500 year sea-
334 level record and wNAO we examined several proxy-based reconstructions of wNAO (Glueck
335 and Stockton, 2001; Cook et al., 2002; Luterbacher et al., 2002; Trouet et al., 2009). The
336 Glueck and Stockton (2001) record is based on data from GISP, and dendrochronological
337 data from Finland to represent the northern pole of the NAO, and many tree ring and
338 precipitation records from the southern pole. The records by Cook et al. (2002) and
339 Luterbacher et al. (2002) are both based on data from a plethora of sites on both sides of the
340 Atlantic. The Trouet et al. (2009) record is based on winter precipitation records from
341 Scotland and February-to-June drought records from Morocco. There are many reasons why
342 proxy records of the NAO may differ (see Trouet et al. (2012) for a review), but we consider
343 the Trouet et al. (2009) reconstruction to be most suitable for comparing with the Iceland sea-
344 level record due to its north-western European northern pole, and the position of Scotland in
345 the dominant wind patterns over the North Atlantic (Fig. 9).

346 In Figure 10 we calculate from our sea-level reconstruction (Fig. 10A) rates of sea-level
347 change (Fig. 10B) and identify three periods of rapid sea-level rise. We arbitrarily define

‘rapid’ as exceeding the average global sea-level rise during the 20th century (1.7mm/yr, Church and White (2006)). The three periods are: AD 1620-1650, when sea-level rise peaked at ~2 mm/yr, and AD 1780-1850 and AD 1950-2000, when maximum sea-level rise was ~3 mm/yr. (These figures are based on the most probable interpretation of the data – see section 3.4.). A comparison with the Trouet et al. (2009) wNAO record (Fig. 10C) shows that the three periods in which the rate of sea-level rise is highest are, within age error, synchronous with strong shifts toward a more positive wNAO. These shifts are by far the largest within the considered time period. Maximum rates of sea-level rise were achieved towards the end of the NAO shifts. The most recent period of rapid sea-level rise (late 20th century) also corresponds with strong shifts towards more positive wNAO in the records by Glueck and Stockton (2001), Cook et al. (2002), and Luterbacher et al. (2002) (Supplementary Fig. 1). Around AD 1800 Luterbacher et al. (2002) also record a marked increase in NAO index (Supplementary Fig. 1). The earliest period of rapid sea-level rise does not seem to have a corresponding signal in NAO records other than the one by Trouet et al. (2009), but others have also found an increased correlation between Atlantic sea level and NAO in more recent centuries (e.g. Andersson, 2002).

From resampling the Trouet et al. (2009) NAO record at the same resolution as a detrended version of our RSL record (Supplementary Fig. 1B), which removes longer wavelength components of sea level, we calculate a coefficient of 0.3 ($p=0.05$) for the correlation between RSL at Viðarhólmi and the NAO (Fig. 11). This suggests a significant influence of NAO on our ~500-year sea level reconstruction, which is the longest record to date on which this is demonstrated.

Our sea-level record shows variability not detected in the record from North Carolina (Kemp et al., 2011) (Supplementary Fig. 1G). This is to be expected given the regionally specific forcing mechanisms of North Atlantic sea levels (Long et al., 2014). For example, along the

Atlantic seaboard of the southeast USA sea levels may be influenced by the strength and position of the Gulf Stream (Ezer et al., 2013, Kopp 2013) and easterly winds are dominant. Reconstructions of North Atlantic overturning circulation strength (e.g. Wanamaker et al., 2012) display little correspondence with our sea-level record.

5.3 West Icelandic sea level and other driving mechanisms

To evaluate the potential of other driving mechanisms we also consider ocean mass changes, GIA, and steric sea-level rise as potential drivers of our Icelandic RSL record. Reductions in ice volume of the Greenland and Antarctic ice sheets and mountain glaciers produce a non-uniform sea-level response, with the largest sea-level rise observed in far-field locations (Mitrovica et al., 2001). Iceland is located too close to Greenland to be sensitive to any potential mass changes of the Greenland Ice Sheet. On the other hand, Iceland is in a far-field location with respect to Antarctica, but the lack of correlation with other North Atlantic sea-level records largely rules out any Antarctic melt signal as a cause of the sea-level variations we reconstructed. Although we cannot completely dismiss contributions from mountain glaciers, the absence of coherent signals in other sea-level proxy records indicates they would have been small or non-existent.

Our field site is quite far from the major ice fields in Iceland and the magnitude of vertical land motion due to changes in ice mass is estimated to have been small in recent times (Árnadóttir et al., 2009) but may have varied in the past. We therefore examined GIA by comparing the timing of the periods of rapid sea-level rise with known changes in local ice load history in Iceland. Regional data exist from AD 1700 onwards (Supplementary Fig. 1H), whereas in the period AD 1400-1700 ice volume changes are largely unconstrained (Kirkbride and Dugmore 2008). The ice body most likely to produce crustal loading (and

hence RSL rise) in the Viðarhólmi region is Langjökull, but data from other regional ice caps and glaciers are reported in Supplementary Fig. 1H for completeness. Of the two major glacial advances reported by Flowers et al. (2007), one coincides with rising and the other with falling sea level in our reconstruction, showing no coherent response of Viðarhólmi sea level to Langjökull mass changes. We therefore reject this as a cause of our reconstructed sea-level variability. Additionally, there is no obvious correlation between our sea-level variability and changes in more distant Icelandic ice masses (Supplementary Fig. 1H), and thus no suggestion these provided the forcing mechanism for this variability.

With regard to thermosteric sea-level rise we hypothesise that reconstructions of sea-surface temperature (SST) and sea-floor temperature (SFT) can be used as a proxy for steric sea level. We compare our record with two SST records and a SFT from marine core MD99-2275 (Supplementary Figs. 1I, J), taken from the North Icelandic Shelf (Knudsen et al., 2004; Ran et al., 2011; Sicre et al., 2011). Our coastal site and this core site are both dominated by Icelandic Coastal Water (Stefánsson and Ólafsson 1991). There is no correspondence between the periods of rapid sea-level change and high SST/SFT, suggesting thermosteric effects on Viðarhólmi sea level are not significant.

6 Conclusions

Only a small number of well-dated late Holocene sea-level reconstructions from the North Atlantic are presently available, and these exhibit patterns that reflect a combination of local and regional signals (e.g. Long et al., 2014). It is important therefore to increase the spatial coverage of well dated sequences and to enhance the resolution of the RSL reconstructions where possible.

419 This study has improved an existing RSL record from Viðarhólmi salt marsh in western
420 Iceland (Gehrels et al., 2006) by adding age control and by developing new quantitative sea-
421 level reconstructions based on diatoms. Its main conclusions are as follows:

422 1) As shown in many other coastal locations, diatoms perform well as a sea-level proxy,
423 due to their high species diversity, strong elevation control and frequent species turnover.

424 2) The careful application of the optimal microfossil group (here, diatoms) can improve
425 RSL reconstructions, but such work must proceed in tandem with the construction of precise
426 age models. We developed a new age model for Viðarhólmi using a combination of AMS
427 ^{14}C dates, ^{137}Cs , geochemical and magnetic markers, as well as a tephra horizons.

428 3) We developed new diatom-based RSL reconstructions, using the modern analogue
429 technique (MAT), to identify and remove samples that have poor contemporary equivalents.
430 After screening our reconstruction shows a ~0.6 m overall (non-GIA corrected) RSL rise
431 since AD 1570, and three episodes of rapid RSL when the rate of rise exceeded 1.7 mm/yr:
432 AD 1620-1650, AD 1780-1850 and AD 1950-2000.

433 4) We hypothesise that Icelandic sea-level variability is controlled by changes in wind
434 patterns associated with shifts in NAO phase based on the strong correlation between a
435 reconstructed NAO index (Trouet et al., 2009) and our detrended RSL record. This result is
436 supported by a positive correlation of the Reykjavik tide-gauge record with regional air
437 pressure and wind speed. NAO-related wind patterns generate set-up on the west coast of
438 Iceland thereby raising local sea level. Taking into account the potential impact of NAO on
439 Icelandic sea level will enhance future predictions of sea-level changes in this region.

440 5) The fluctuating nature of the Icelandic RSL record contrasts with other records from
441 the North Atlantic and highlights the importance of regionally specific driving mechanisms
442 over centennial timescales.

8 Acknowledgements

This research was funded by the Natural Environment Research Council (grant no. NE/G003440/1). Radiocarbon dating was performed with help from the Natural Environment Research Council Radiocarbon Committee (allocations 1490.0810 and 1604.0112). Tephrochronology was performed with support from the Tephrochronology Analytical Unit (allocation TAU71/1011). We thank James Scourse and an anonymous reviewer for their constructive comments. We thank Chris Hayward and Donald Herd for help with the tephra analyses, and Gudrun Larsen for advice and for a reference sample of Katla 1721 ash. We thank the Icelandic Met Office for supplying climate data. We thank Peter Schmidt and Björn Lund for advice on GIA and William Marshall for assistance in the field. The paper is a contribution to IGCP project 588 (“Preparing for Coastal Change”) and to PALSEA2 (an INQUA International Focus Group and a PAGES working group).

- 458 Andersson, H.C., 2002. Influence of long-term regional and large-scale atmospheric
459 circulation on the Baltic sea level. *Tellus A* 54, 76-88.
- 460 Angelier, J., Slunga, R., Bergerat, F., Stefansson, R., Homberg, C., 2004. Perturbation of
461 stress and oceanic rift extension across transform faults shown by earthquake focal
462 mechanisms in Iceland. *Earth Planet. Sci. Lett.* 219, 271-284.
- 463 Angell, J.K., Korshover, T., 1974. Quasi-Biennial and Long-Term Fluctuations in the Centers
464 of Action. *Mon. Weath. Rev.* 102, 669-678.
- 465 Árnadóttir, T., Lund, B., Jiang, W., Geirsson, H., Björnsson, H., Einarsson, P., Sigurdsson, T.,
466 2009. Glacial rebound and plate spreading: results from the first countrywide GPS
467 observations in Iceland. *Geophys. J. Int.* 177, 691-716.
- 468 Barlow, N.L.M., Shennan, I., Long, A.J., 2012. Relative sea-level response to Little Ice Age
469 ice mass change in south central Alaska: Reconciling model predictions and geological
470 evidence. *Earth Planet. Sci. Lett.* 315–316, 62-75.
- 471 Barlow, N.L.M., Shennan, I., Long, A.J., Gehrels, W.R., Saher, M.H., Woodroffe, S.A.,
472 Hillier, C., 2013. Salt marshes as late Holocene tide gauges. *Glob. Planet. Change* 106,
473 90-110.
- 474 Barlow, N.L.M., Long, A.J., Saher, M.H., Gehrels, W.R., Garnett, M.H., Scaife, R.G., 2014.
475 Salt-marsh reconstructions of relative sea-level change in the North Atlantic during the
476 last 2000 years. *Quat. Sci. Rev.* 99, 1-16.
- 477 Birks, H.J.B., Line, J.M., Juggins, S., Stevenson, A.C., Braak, C.J.F.T., 1990. Diatoms and
478 pH reconstruction. *Phil. Trans. Roy. Soc. Lond. B, Biol. Sci.* 327, 263-278.
- 479 Björnsson, H., 1979. Glaciers in Iceland. *Jökull* 29, 74-80.
- 480 Blaauw, M., Christen, J.A., 2011. Flexible paleoclimate age-depth models using an
481 autoregressive gamma process. *Bayesian Anal.* 6, 457-474.
- 482 Brain, M.J., Long, A.J., Woodroffe, S.A., Petley, D.N., Milledge, D.G., Parnell, A.C., 2012.
483 Modelling the effects of sediment compaction on salt marsh reconstructions of recent
484 sea-level rise. *Earth. Planet. Sci. Letts.* 345–348, 180-193.
- 485 Bronk Ramsey, C., Gigham, T., Leach, P., 2004. Towards high-precision AMS; progress and
486 limitations. *Radiocarbon* 46, 17-24.
- 487 Carleton, A.M., 1988. Meridional Transport of Eddy Sensible Heat in Winters Marked by
488 Extremes of the North Atlantic Oscillation, 1948/49–1979/80. *J. Clim.* 1, 212-223.
- 489 Charman, D.J., Gehrels, W.R., Manning, C., Sharma, C., 2010. Reconstruction of recent sea-
490 level change using testate amoebae. *Quat. Res.* 73, 208-219.
- 491 Church, J.A., White, N.J., 2006. A 20th century acceleration in global sea-level rise. *Geophys.*
492 *Res. Lett.* 33. L01602, doi:10.1029/2005GL024826.
- 493 Compo, G.P., Whitaker, J.S., Sardeshmukh, P.D., Matsui, N., Allan, R.J., Yin, X., Gleason,
494 B.E., Vose, R.S., Rutledge, G., Bessemoulin, P., Brönnimann, S., Brunet, M.,
495 Crouthamel, R.I., Grant, A.N., Groisman, P.Y., Jones, P.D., Kruk, M.C., Kruger, A.C.,
496 Marshall, G.J., Maugeri, M., Mok, H.Y., Nordli, Ø., Ross, T.F., Trigo, R.M., Wang,
497 X.L., Woodruff, S.D., Worley, S.J., 2011. The Twentieth Century Reanalysis Project.
498 *Quart. J. Roy. Meteorol. Soc.* 137, 1-28.
- 499 Cook, E.R., D'Arrigo, R.D., Mann, M.E., 2002. A well-verified, multiproxy reconstruction of
500 the Winter North Atlantic Oscillation Index since A.D. 1400. *J. Clim.* 15, 1754-1764.
- 501 Cornes, R.C., Jones, P.D., Briffa, K.R., Osborn, T.J., 2013. Estimates of the North Atlantic
502 Oscillation back to 1692 using a Paris–London westerly index. *Int. J. Climat.* 33, 228-
503 248.

Davies, S.M., Elmquist, M., Bergman, J., Wohlfarth, B., Hammarlund, D., 2007.
 Cryptotephra sedimentation processes within two lacustrine sequences from west
 central Sweden. *The Holocene* 17, 319-330.

De Rijk, S., 1995. Agglutinated foraminifera as indicators of salt-marsh development in
 relation to late Holocene sea level rise (Great Marshes at Barnstable, Massachusetts).
 PhD thesis, Free University, Amsterdam, Netherlands.

Douglas, B.C., 2008. Concerning evidence for fingerprints of glacial melting. *J. Coast. Res.*
 24, 218-227.

Einarsson, E.H., Larsen, G., Pórarinnsson, S., 1980. The Sólheimar tephra layer and the Katla
 eruption of 1357. *Acta Naturalia Islandica* 28, 1-24.

Einarsson, M.A., 1984. Climate of Iceland. *World Survey of Climatology* 15, 673-697.

Ezer, T., Atkinson, L.P., Corlett, W.B., Blanco, J.L., 2013. Gulf Stream's induced sea level
 rise and variability along the U.S. mid-Atlantic coast. *J. Geophys. Res. Oceans* 118,
 685-697.

Flowers, G.E., Björnsson, H., Geirsdóttir, Á., Miller, G.H., Clarke, G.K.C., 2007. Glacier
 fluctuation and inferred climatology of Langjökull ice cap through the Little Ice Age.
Quat. Sci. Rev. 26, 2337-2353.

Foged, N., 1974. Freshwater diatoms in Iceland. *Bibliotheca Phycologica* 15, 1-118.

Frankcombe, L.M., Dijkstra, H.A., 2009. Coherent multidecadal variability in North Atlantic
 sea level. *Geophys. Res. Lett.* 36, L15604, doi:10.1029/2009GL039455.

Gehrels, W.R., 1999. Middle and Late Holocene sea-level changes in eastern Maine
 reconstructed from foraminiferal saltmarsh stratigraphy and AMS ¹⁴C dates on basal
 peat. *Quat. Res.* 52, 350-359.

Gehrels, W.R., Belknap, D.F., Black, S., Newnham, R.M., 2002. Rapid sea-level rise in the
 Gulf of Maine, USA, since AD 1800. *The Holocene* 12, 383-389.

Gehrels, W.R., Marshall, W.A., Gehrels, M.J., Larsen, G., Kirby, J.R., Eiriksson, J.,
 Heinemeier, J., Shimmield, T., 2006. Rapid sea-level rise in the North Atlantic Ocean
 since the first half of the nineteenth century. *The Holocene* 16, 949-965.

Gehrels, W.R., Milne, G.A., Kirby, J.R., Patterson, R.T., Belknap, D.F., 2004. Late Holocene
 sea-level changes and isostatic crustal movements in Atlantic Canada. *Quat. Int.* 120,
 79-89.

Gehrels, W.R., Roe, H.M., Charman, D.J., 2001. Foraminifera, testate amoebae and diatoms
 as sea-level indicators in UK saltmarshes: a quantitative multiproxy approach. *J. Quat.*
Sci. 16, 201-220.

Gehrels, W.R., Woodworth, P.L., 2013. When did modern rates of sea-level rise start? *Glob.*
Planet. Change. 100, 263-277.

Glueck, M.F., Stockton, C.W., 2001. Reconstruction of the North Atlantic Oscillation, 1429–
 1983. *Int. J. Climatol.* 21, 1453-1465.

Haflidason, H., Eiriksson, J., Kreveld, S.V., 2000. The tephrochronology of Iceland and the
 North Atlantic region during the Middle and Late Quaternary: a review. *J. Quat. Sci.* 15,
 3-22.

Haflidason, H., Larsen, G., Ólafsson, G., 1992. The Recent Sedimentation History of
 Thingvallavatn, Iceland. *Oikos* 64, 80-95.

Haigh, I., Nicholls, R., Wells, N., 2010. Assessing changes in extreme sea levels: Application
 to the English Channel, 1900–2006. *Cont. Shelf Res.* 30, 1042-1055.

Hameed, S., Piontkovski, S., 2004. The dominant influence of the Icelandic Low on the
 position of the Gulf Stream northwall. *Geophys. Res. Lett.* 31, L09303.

Hartley, B., Barber, H.G., Carter, J.R., 1996. *An Atlas of British Diatoms*. Biopress, Bristol,
 601 pp

553 Hayward, C., 2012. High spatial resolution electron probe microanalysis of tephra and melt
554 inclusions without beam-induced chemical modification. *The Holocene* 22, 119-125.

555 Hemphill-Haley, E., 1993. Taxonomy of recent and fossil (Holocene) diatoms
556 (Bacillariophyta) from northern Willapa Bay, Washington. U.S. Department of the
557 Interior, US Geological Survey, 151 pp.

558 Hong, B.G., Sturges, W., Clarke, A.J., 2000. Sea Level on the U.S. East Coast: decadal
559 variability caused by open ocean wind-curl forcing. *J. Phys. Ocean.* 30, 2088-2098.

560 Hurrell, J., Van Loon, H., 1997. Decadal variations in climate associated with the North
561 Atlantic Oscillation. *Clim. Chan.* 36, 301-326.

562 Hurrell, J.W., Kushnir, Y., Ottersen, G., Visbeck, M., 2003. An overview of the North
563 Atlantic oscillation. *Geophys. Mon. Amer. Geophys. Union* 134, 1-36.

564 Hustedt, F., 1953. Die Systematik der Diatomeen in ihren Beziehungen zur Geologie und
565 Ökologie nebst einer Revision des Halobien-systems. *Svensk Botanisk Tidskrift* 47,
566 509-519.

567 Ingólfsson, Ó., Norddahl, H., 2001. High relative sea level during the Bolling Interstadial in
568 western Iceland: A reflection of ice-sheet collapse and extremely rapid glacial
569 unloading. *Arct. Antar. Alp. Res.* 231-243.

570 Jackson, S.T., Williams, J.W., 2004. Modern analogs in Quaternary paleoecology: here today,
571 gone yesterday, gone tomorrow? *Ann. Rev. Earth Planet. Sci.* 32, 495-537.

572 Jevrejeva, S., Grinsted, A., Moore, J.C., Holgate, S., 2006. Nonlinear trends and multiyear
573 cycles in sea level records. *J. Geophys. Res.* 111, C09012, doi:10.1029/2005JC003229.

574 Jevrejeva, S., Moore, J.C., Grinsted, A., 2008. Relative importance of mass and volume
575 changes to global sea level rise. *J. Geophys. Res.* 113, D08105,
576 doi:10.1029/2007JD009208.

577 Jones, P.D., Jonsson, T., Wheeler, D., 1997. Extension to the North Atlantic oscillation using
578 early instrumental pressure observations from Gibraltar and south-west Iceland. *Int. J.*
579 *Climat.* 17, 1433-1450.

580 Juggins, S., 2003. C2 user guide. Software for ecological and palaeoecological data analysis
581 and visualisation. University of Newcastle, Newcastle upon Tyne, UK.

582 Kemp, A.C., Horton, B.P., Corbett, D.R., Culver, S.J., Edwards, R.J., van de Plassche, O.,
583 2009. The relative utility of foraminifera and diatoms for reconstructing late Holocene
584 sea-level change in North Carolina, USA. *Quat. Res.* 71, 9-21.

585 Kemp, A.C., Horton, B.P., Donnelly, J.P., Mann, M.E. Vermeer, M., Rahmstorf, S., 2011.
586 Climate related sea-level variations over the past two millennia. *Proc. Nat. Acad. Sci.*
587 108, 11017-11022.

588 Kemp, A.C., Horton, B.P., Vane, C.H., Bernhardt, C.E., Corbett, D.R., Engelhart, S.E.,
589 Anisfeld, S.C., Parnell, A.C., Cahill, N., 2013. Sea-level change during the last 2500
590 years in New Jersey, USA. *Quat. Sci. Rev.* 81, 90-104.

591 Kirkbride, M.P., Dugmore, A.J., 2008. Two millennia of glacier advances from southern
592 Iceland dated by tephrochronology. *Quat. Res.* 70, 398-411.

593 Knudsen, K.L., Eiríksson, J., Jansen, E., Jiang, H., Rytter, F., Gudmundsdóttir, R.E., 2004.
594 Palaeoceanographic changes off North Iceland through the last 1200 years:
595 foraminifera, stable isotopes, diatoms and ice rafted debris. *Quat. Sci. Rev.* 23, 2231-
596 2246.

597 Kolker, A.S., Hameed, S., 2007. Meteorologically driven trends in sea level rise. *Geophys.*
598 *Res. Lett.* 34, L23616.

599 Kopp, R.E., 2013. Does the mid-Atlantic United States sea level acceleration hot spot reflect
600 ocean dynamic variability? *Geophys. Res. Lett.* 40, 3981-3985.

601 Larsen, G., 2000. Holocene eruptions within the Katla volcanic system, south Iceland:
602 Characteristics and environmental impact. *Jökull* 49, 1-28.

- Long, A.J., Woodroffe, S.A., Milne, G.A., Bryant, C.L., Simpson, M.J.R., Wake, L.M., 2012. Relative sea-level change in Greenland during the last 700 yrs and ice sheet response to the Little Ice Age. *Earth Planet. Sci. Letts.* 315–316, 76-85.
- Long, A.J., Barlow, N.L.M., Gehrels, W.R., Saher, M.H., Woodworth, P.L., Scaife, R.G., Brain, M.J., Cahill, N., 2014. Contrasting records of sea-level change in the eastern and western North Atlantic during the last 300 years. *Earth Planet. Sci. Lett.* 388, 110-122.
- Luterbacher, J., Schmutz, C., Gyalistras, D., Xoplaki, E., Wanner, H., 1999. Reconstruction of monthly NAO and EU indices back to AD 1675. *Geophys. Res. Lett.* 26, 2745-2748.
- Luterbacher, J., Xoplaki, E., Dietrich, D., Jones, P.D., Davies, T.D., Portis, D., Gonzalez-Rouco, J.F., von Storch, H., Gyalistras, D., Casty, C., Wanner, H., 2001. Extending North Atlantic oscillation reconstructions back to 1500. *Atmos. Sci. Lett.* 2, 114-124.
- Miller, L., Douglas, B.C., 2007. Gyre-scale atmospheric pressure variations and their relation to 19th and 20th century sea level rise. *Geophys. Res. Lett.* 34., L16602, doi:10.1029/2007GL030862.
- Milne, G.A., Gehrels, W.R., Hughes, C.W., Tamisiea, M.E., 2009. Identifying the causes of sea-level change. *Nat. Geosci.* 2, 471 - 478.
- Mitrovica, J.X., Tamisiea, M.E., Davis, J.L., Milne, G.A., 2001. Recent mass balance of polar ice sheets inferred from patterns of global sea-level change. *Nature* 409, 1026-1029.
- Óladóttir, B., Sigmarsson, O., Larsen, G., Thordarson, T., 2008. Katla volcano, Iceland: magma composition, dynamics and eruption frequency as recorded by Holocene tephra layers. *Bulletin of Volcanology* 70, 475-493.
- Overpeck, J.T., Webb III, T., Prentice, I.C., 1985. Quantitative interpretation of fossil pollen spectra: Dissimilarity coefficients and the method of modern analogs. *Quat. Res.* 23, 87-108.
- Palmer, A.J., Abbott, W.H., 1986. Diatoms as indicators of sea level change. In: Van de Plassche, O. (Ed.), *Sea Level Research: a Manual for the Collection and Evaluation of Data*. Geobooks, Norwich, pp. 457-488.
- Patterson, R.T., Hutchinson, I., Guilbault, J.P., Clague, J.J., 2000. A comparison of the vertical zonation of diatom, foraminifera, and macrophyte assemblages in a coastal marsh; implications for greater paleo-sea level resolution. *Micropaleontology* 46, 229-244.
- Ponte, R.M., 1992. The sea level response of a stratified ocean to barometric pressure forcing. *J. Phys. Oceanogr.* 22, 109-113.
- Ran, L., Jian, g H., Knudsen, K.L., Eiríksson, J., 2011. Diatom-based reconstruction of palaeoceanographic changes on the North Icelandic shelf during the last millennium. *Palaeogeog. Palaeoclim. Palaeoecol.* 302, 109-119.
- Reimer, P.J., Baillie, M.G.L., Bard, E., Bayliss, A., Beck, J.W., Blackwell, P.G., Ramsey, C.B., Buck, C.E., Burr, G.S., Edwards, R.L., Friedrich, M., Grootes, P.M., Guilderson, T.P., Hajdas, I., Heaton, T.J., Hogg, A.G., Hughen, K.A., Kaiser, K.F., Kromer, B., McCormac, F.G., Manning, S.W., Reimer, R.W., Richards, D.A., Southon, J.R., Talamo, S., Turney, C.S.M., van der Plicht, J., Weyhenmeyer, C.E., 2009. IntCal09 and Marine09 radiocarbon age calibration curves, 0-50,000 years cal BP. *Radiocarbon* 51, 1111-1150.
- Reimer, P., Bard, E., Bayliss, A., Beck, J., Blackwell, P., Bronk Ramsey, C., Buck, C., Cheng H., Edwards, R., Friedrich, M., Grootes, P., Guilderson, T., Hafliðason, H., Hajdas, I., Hatté, C., Heaton, T., Hogg, A., Hughen, K., Kaiser, K., Kromer, B., Manning, S., Niu, M., Reimer, R., Richards, D., Scott, E., Southon, J., Turney, C., van der Plicht, J., 2013.

652 IntCal13 and MARINE13 radiocarbon age calibration curves 0-50000 years cal BP.
 653 Radiocarbon 55, 1869-1887.
 654 Sahsamanoglou, H.S., 1990. A contribution to the study of action centres in the North
 655 Atlantic. *Int. J. Climatol.* 10, 247-261.
 656 Serreze, M.C., Carse, F., Barry, R.G., Rogers, J.C., 1997. Icelandic Low cyclone activity:
 657 climatological features, linkages with the NAO, and relationships with recent changes
 658 in the Northern Hemisphere circulation. *J. Climate* 10, 453-464.
 659 Sicre, M.A., Hall, I.R., Mignot, J., Khodri, M., Ezat, U., Truong, M.X., Eiríksson, J.,
 660 Knudsen, K.L., 2011. Sea surface temperature variability in the subpolar Atlantic over
 661 the last two millennia. *Paleoceanography* 26, PA4218, doi:10.1029/2011PA002169,
 662 Sigurgeirsson, M.A., 1992. Gjoskumyndanir a Reykjanesi. MSc Thesis, University of Iceland,
 663 113 pp.
 664 Simpson, G.L., 2007. Analogue methods in palaeoecology: using the analogue package. *J.*
 665 *Stat. Software* 22, 1-29.
 666 Stefánsson, U., Ólafsson, J., 1991. Nutrients and fertility of Icelandic waters. *Rit Fiskideild.* 7,
 667 1-56.
 668 Ter Braak, C.J.F., Juggins, S., 1993. Weighted averaging partial least squares regression
 669 (WA-PLS): an improved method for reconstructing environmental variables from
 670 species assemblages. *Hydrobiologia* 269-270, 485-502.
 671 Ter Braak, C.J.F., Prentice, I.C., 1988. A theory of gradient analysis. *Adv. Ecol. Res.* 34.
 672 Ter Braak, C.J.F., Smilauer, P., 2002. CANOCO reference manual and CanoDraw for
 673 Windows user's guide: software for canonical community ordination (version 4.5).
 674 Thorarinsson, S., 1974. Vötnin stríð (the fast flowing rivers). Saga Skeiðarárhlaupa og
 675 Grímsvatnagosa. Bókaútgáfa Menningarsjóðs, Reykjavík. 254 pp.
 676 Trouet, V., Esper, J., Graham, N.E., Baker, A., Scourse, J.D., Frank, D.C., 2009. Persistent
 677 Positive North Atlantic Oscillation Mode Dominated the Medieval Climate Anomaly.
 678 *Science* 324, 78-80.
 679 Trouet, V., Scourse, J.D., Raible, C.C., 2012. North Atlantic storminess and Atlantic
 680 Meridional Overturning Circulation during the last Millennium: reconciling
 681 contradictory proxy records of NAO variability. *Glob. Planet. Change* 84-85, 48-55.
 682 Tsimplis, M.N., Shaw, A.G.P., Flather, R.A., Woolf, D.K., 2006. The influence of the North
 683 Atlantic Oscillation on the sea-level around the northern European coasts reconsidered:
 684 the thermosteric effects. *Phil. Trans. Roy. Soc. A* 364, 845-856.
 685 Tsimplis, M.N., Woolf, D.K., Osborn, T.J., Wakelin, S., Wolf, J., Flather, R., Shaw, A.G.P.,
 686 Woodworth, P., Challenor, P., Blackman, D., Pert, F., Yan, Z., Jevrejeva, S., 2005.
 687 Towards a vulnerability assessment of the UK and northern European coasts: the role of
 688 regional climate variability. *Phil. Trans. Roy. Soc. A* 363, 1329-1358.
 689 Van de Plassche, O., 2000. North Atlantic climate-ocean variations and sea level in Long
 690 Island Sound, Connecticut, since 500 cal yr A.D. *Quat. Res.* 53, 89-97.
 691 Vos, P.C., de Wolf, H., 1993. Diatoms as a tool for reconstructing sedimentary environments
 692 in coastal wetlands; methodological aspects. *Hydrobiologia* 269, 285-296.
 693 Wakelin, S.L., Woodworth, P.L., Flather, R.A., Williams, J.A., 2003. Sea-level dependence
 694 on the NAO over the NW European Continental Shelf. *Geophys. Res. Letts.* 30, 1403.
 695 Wanamaker, A.D.J., Butler, P.G., Scourse, J.D., Heinemeier, J., Eiríksson, J., Knudsen,
 696 K.L., Richardson, C.A., 2012. Surface changes in the North Atlantic meridional
 697 overturning circulation during the last millennium. *Nat. Comm.* 3, 899.
 698 Ward, P.L., 1971. New interpretation of the geology of Iceland. *Geol. Soc. America Bull.* 82,
 699 2991-3012.
 700 Watcham, E.P., Shennan, I., Barlow, N.L.M., 2013. Scale considerations in using diatoms as
 701 indicators of sea-level change: lessons from Alaska. *J. Quat. Sci.* 28, 165-179.

702 Van der Werff, A., Huls, H., 1957-1974. *Diatomeeënflora van Nederland*, Reprinted 1976.
703 Otto Koeltz Science Publishers, Koenigstein. West Germany.
704 Woodworth, P.L., Flather, R.A., Williams, J.A., Wakelin, S.L., Jevrejeva, S., 2007. The
705 dependence of UK extreme sea levels and storm surges on the North Atlantic
706 Oscillation. *Cont. Shelf Res.* 27, 935-946.
707 Woolf, D.K., Shaw, A.G., Tsimplis, M.N., 2003. The influence of the North Atlantic
708 Oscillation on sea-level variability in the North Atlantic region. *The Glob. Atmos.*
709 *Ocean Syst.* 9, 145-167. Wunsch, C., Stammer, D., 1997. Atmospheric loading and the
710 oceanic “inverted barometer” effect. *Rev. of Geophys.* 35, 79-107.

711 **Figure captions**

712 **Fig. 1.** Location map and previous work. A: Regional map showing location of study site
713 (Viðarhólmi) and other locations mentioned in text. B: Aerial photograph of Viðarhólmi salt
714 marsh showing location of surface sample transects (T1-4) and sampled section V3A. C:
715 Foraminifera-based sea-level reconstruction for Viðarhólmi salt marsh, with 2σ error bars,
716 spanning the last 2000 years from Gehrels et al. (2006).

717 **Fig. 2.** Stratigraphy and sedimentological data of section V3A, showing dry bulk density
718 (DBD), grain-size fractions and lithology (including dated tephras).

719 **Fig. 3** Transfer function model details. A: Scatter plot of observed *versus* model-predicted
720 elevations of modern diatom samples shown in Fig. 5. B: Residuals (predicted minus
721 observed sample elevations). RMSEP – root mean squared error of prediction.

722 **Fig. 4** Age model and output files computed by the software package Bacon (Blaauw and
723 Christen, 2011) for section V3A. A: Age-depth model based on ^{14}C (purple) and other
724 (turquoise) dates. The red curve shows the weighted mean ages of all depths, whereas
725 greyscales show uncertainties (where darker grey indicates more certain sections). B: Stable
726 Markov Chain Monte Carlo run. C: Prior (green curve; gamma distribution with mean 20,
727 shape 3) and posterior (grey histogram) distributions for the accumulation rate (yr/cm). D:
728 Prior (green curve; beta distribution with strength 3 and mean 0.1) and posterior (grey
729 histogram) for the memory. Section sizes were set at 5 mm.

730 **Fig. 5** The vertical distribution of the main species of diatoms, shown for species greater than
731 5% of total valves counted. Diatom classification according to Vos and de Wolf (1993). P
732 (blue): Polyhalobian; M (green): Mesohalobian (brackish); O-h (light orange):

733 Oligohalobian-halophilous; O-i (dark orange): Oligohalobian-indifferent; H (red):

734 Halophobous. MSL - mean sea level.

735 **Fig. 6** Fossil assemblages of the main species of diatoms used as sea-level proxies. Diatoms
736 shown for species greater than 5% of total valves counted. Diatom classification as in Fig. 5.
737 Palaeo-marsh surface elevations (PMSE) are also shown. Samples with good/close modern
738 analogues are shown as solid circles. Samples with poor modern analogues are shown as
739 open circles.

740 **Fig. 7** New relative sea-level reconstruction for western Iceland based on diatoms. A: New
741 reconstruction for the last half millennium. Black crosses are data point from levels that were
742 directly dated. Grey crosses are data points for which ages are estimated from the age model
743 (Fig. 4). Superimposed is the Reykjavik tide-gauge record (www.psmsl.org). B: Composite
744 RSL reconstruction for western Iceland, combining the diatom-based reconstruction for the
745 last 500 years (this paper) and the foraminifera-based reconstruction for the older part of the
746 record (Gehrels et al., 2006).

747 **Fig. 8** Annual winter mean time series of air pressure, wind speed, wind direction, and NAO
748 index, averaged for the box shown in Fig. 9 over the period 1871-2011. Mean sea level (MSL)
749 at Reykjavik is shown as red lines. Upper panels (A-D) show annual data and lower panels
750 (E-H) show 9-year running averages. Note that the vertical axes in panels A and E are
751 reversed compared to the other panels.

752 **Fig. 9** Detrended mean sea-level (MSL) recorded at Reykjavik, showing sea levels
753 subdivided into four height categories: >1 standard deviation (very high), 0-1 standard
754 deviation (high), -1-0 standard deviation (low), and <-1 standard deviation (very low). Maps
755 show the average air pressure, wind speed and wind direction for each of the four height
756 categories. The box shows the area used to calculate parameters shown in Fig. 8.

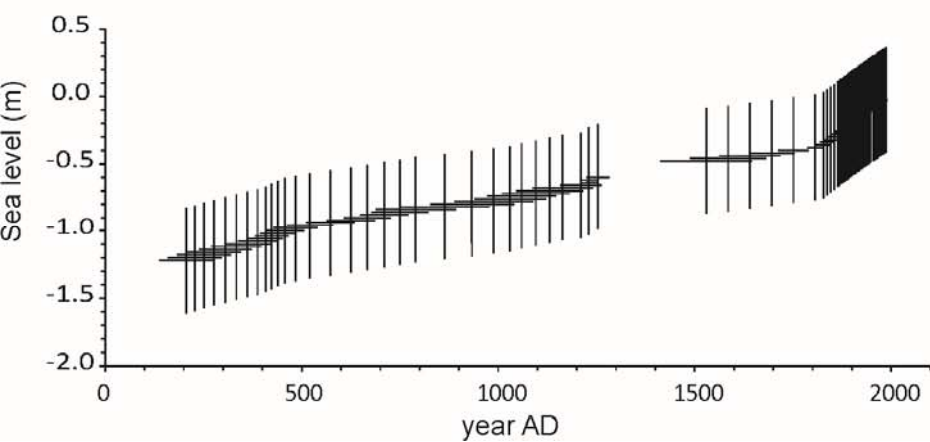
Fig. 10 Comparison of our sea-level reconstruction with the NAO proxy record of Trouet et al. (2009). A: Sea-level reconstruction for western Iceland. The envelope represents the 68% confidence limits calculated from chronological and height errors of data points. B: Rates of sea-level change for the Icelandic sea-level reconstruction in panel A. The envelope shows 68% confidence limits and the line represents the most probably reconstruction. The grey vertical bars show the three periods where this line exceeds the 20th century average of 1.7 mm/yr (Church and White 2006). C: The reconstructed NAO index of Trouet et al. (2009).

Fig. 11 Scatter plot showing the correlation between the detrended sea-level proxy data from western Iceland (see Supplementary Figure 1B) and the reconstructed NAO index (Trouet et al., 2009).

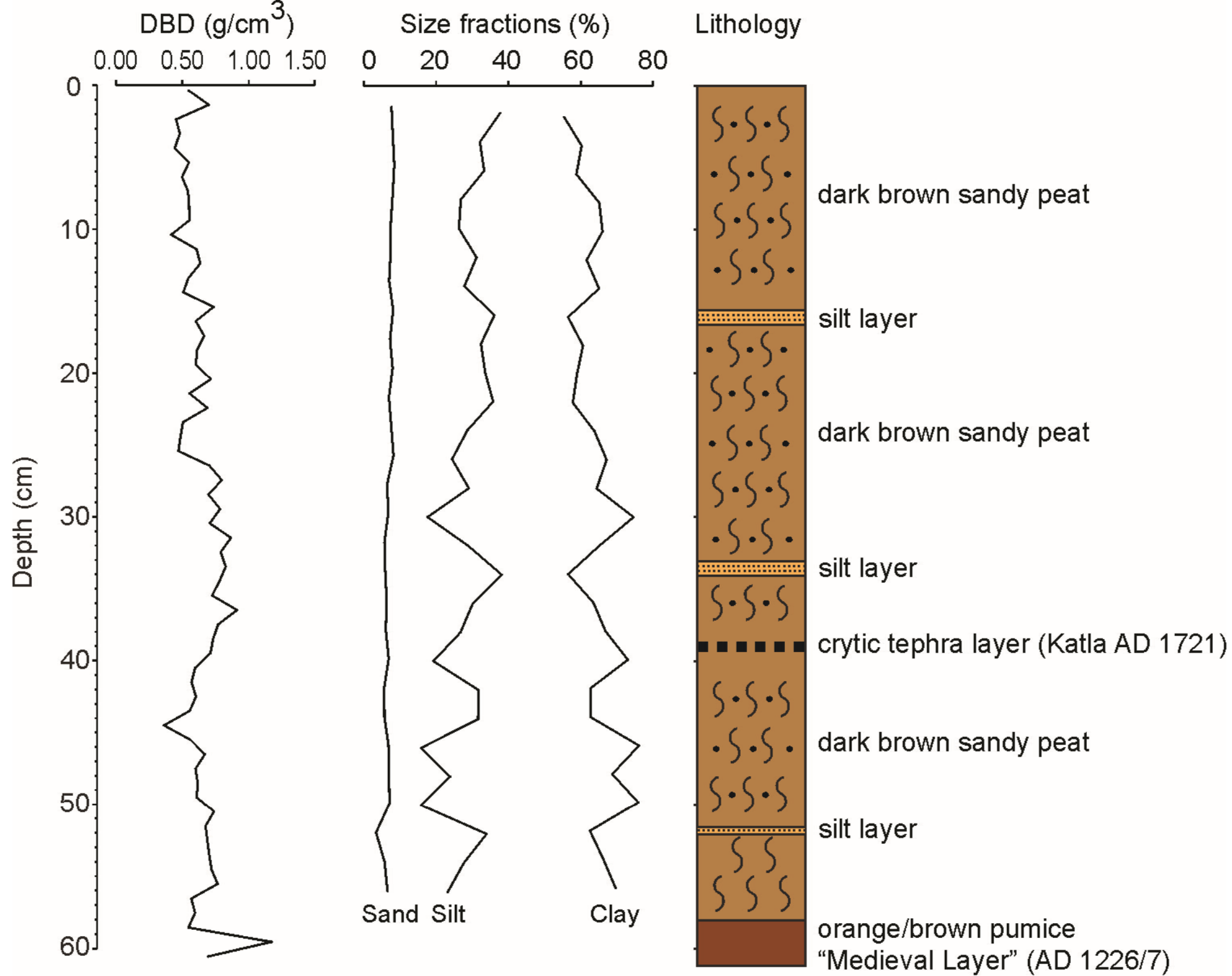
Table captions

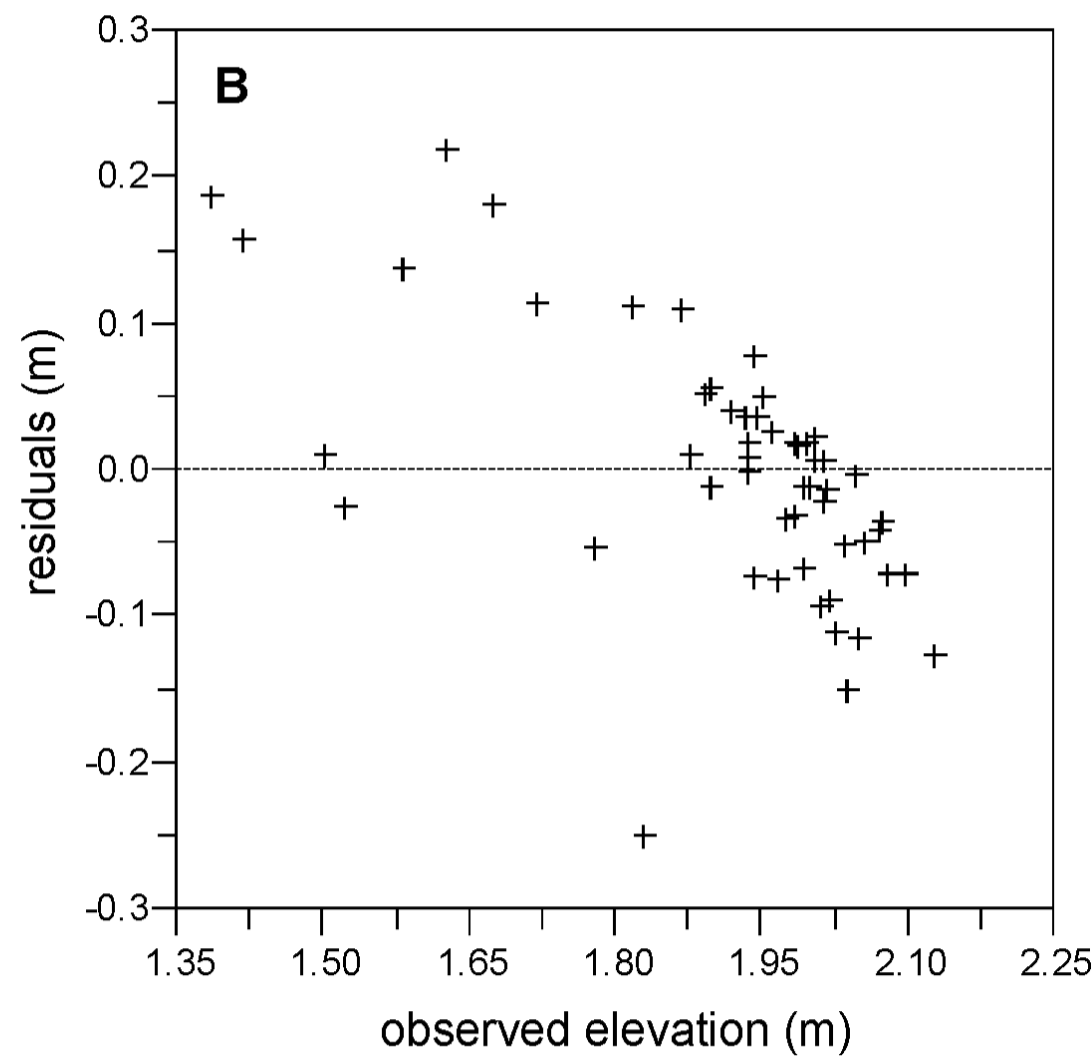
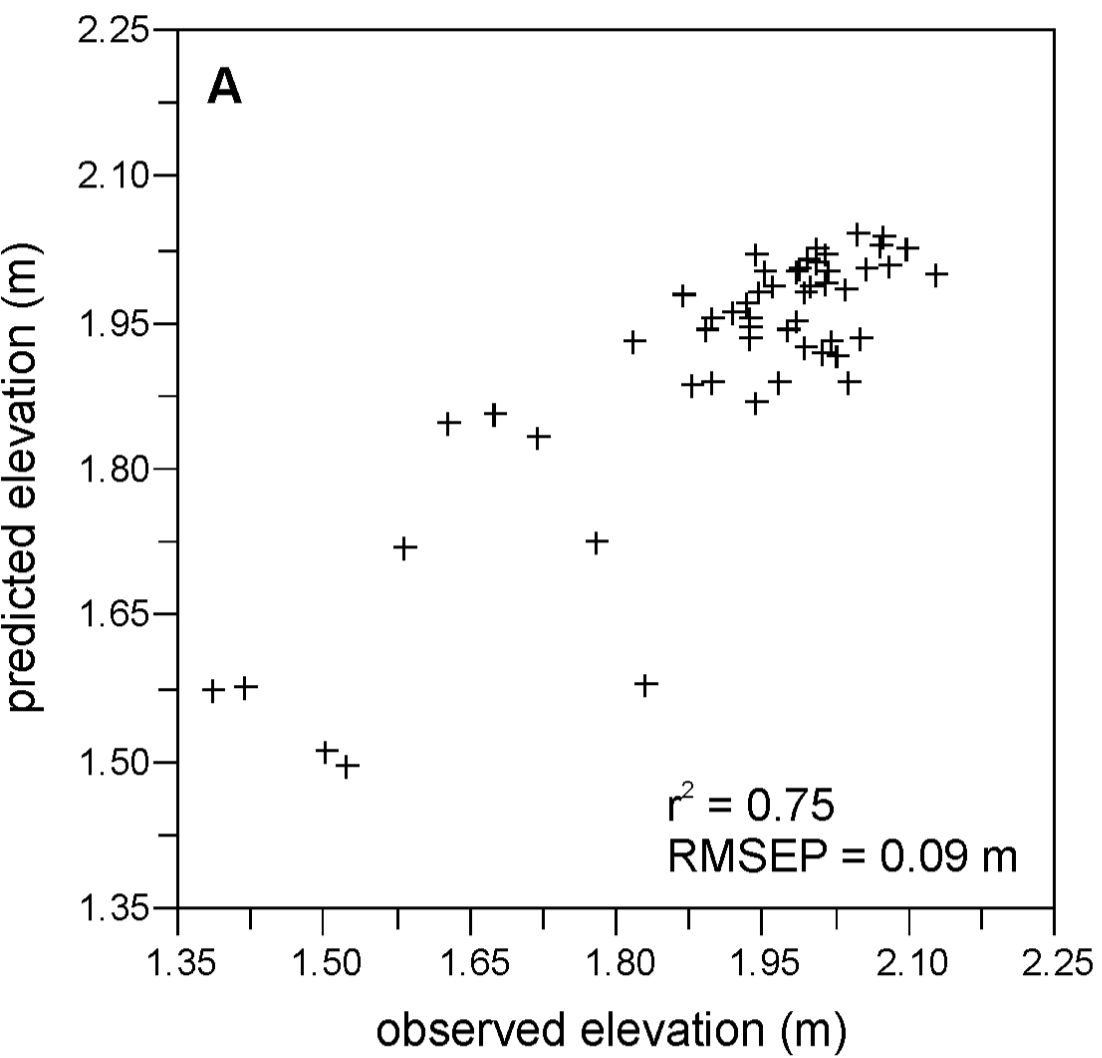
Table 1 Age-depth data used to reconstruct relative sea-level changes in western Iceland during the last 500 years. Sources: 1 - this study; 2 - Gehrels et al. (2006).

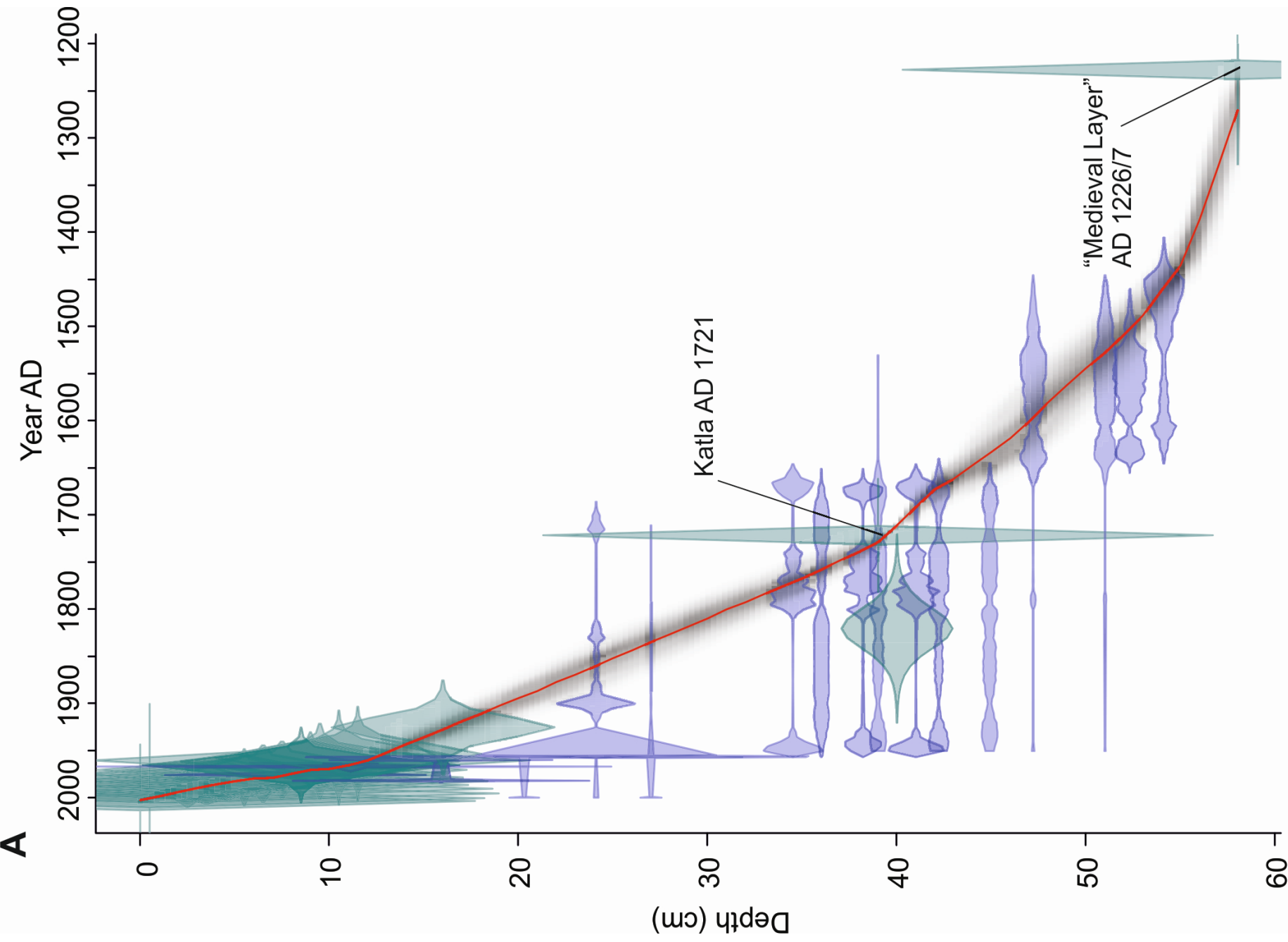
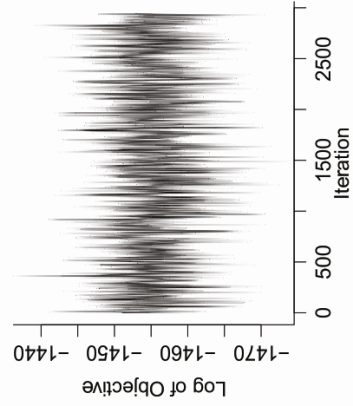
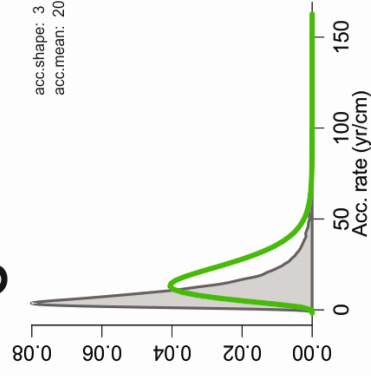
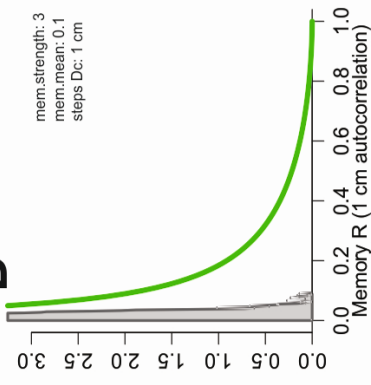
Table 2 Icelandic sea-level data for the last 500 years. I.M. – indicative meaning. MSL – mean sea level. Relative sea level (RSL) positions are given relative to present sea level (i.e. 0 m).

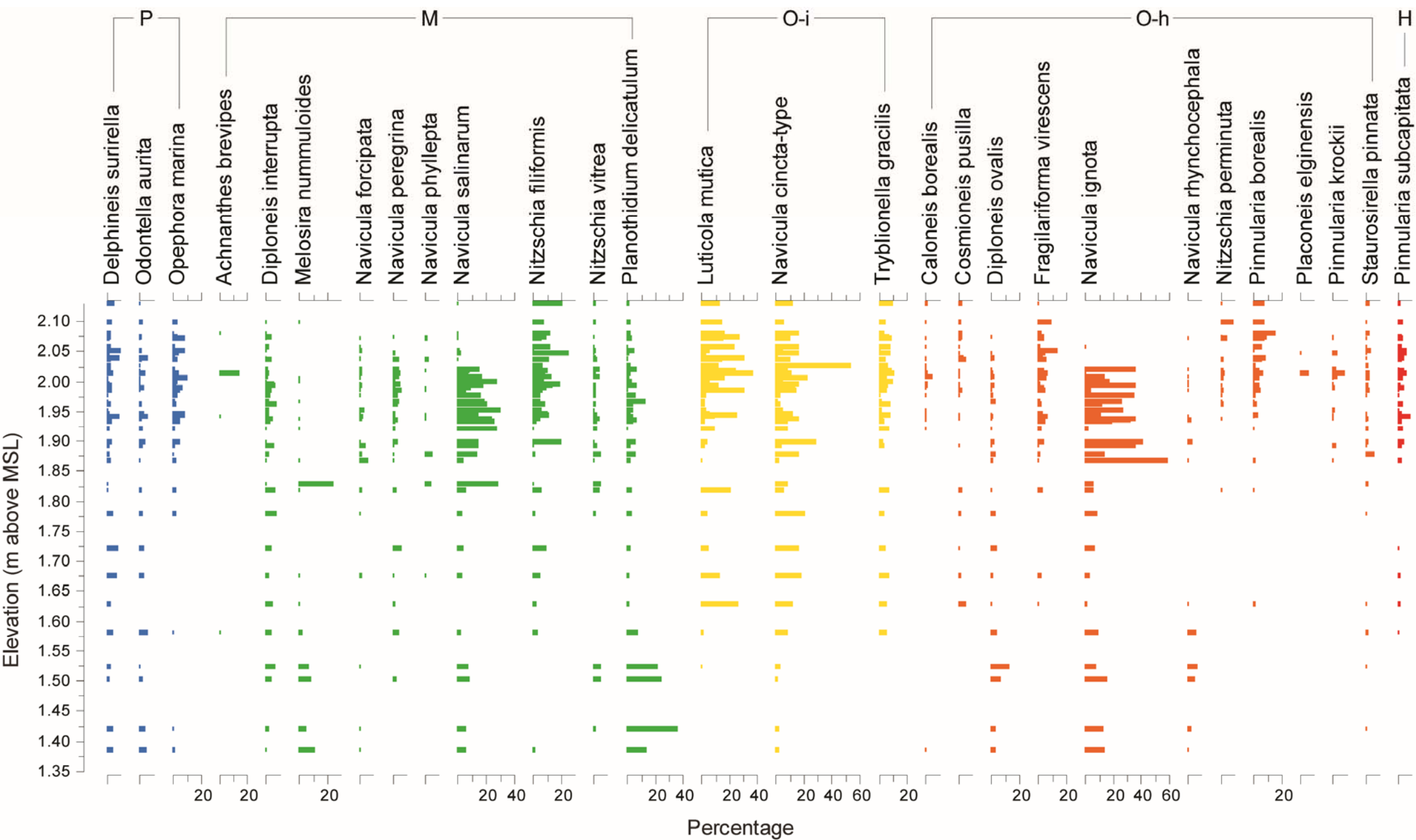


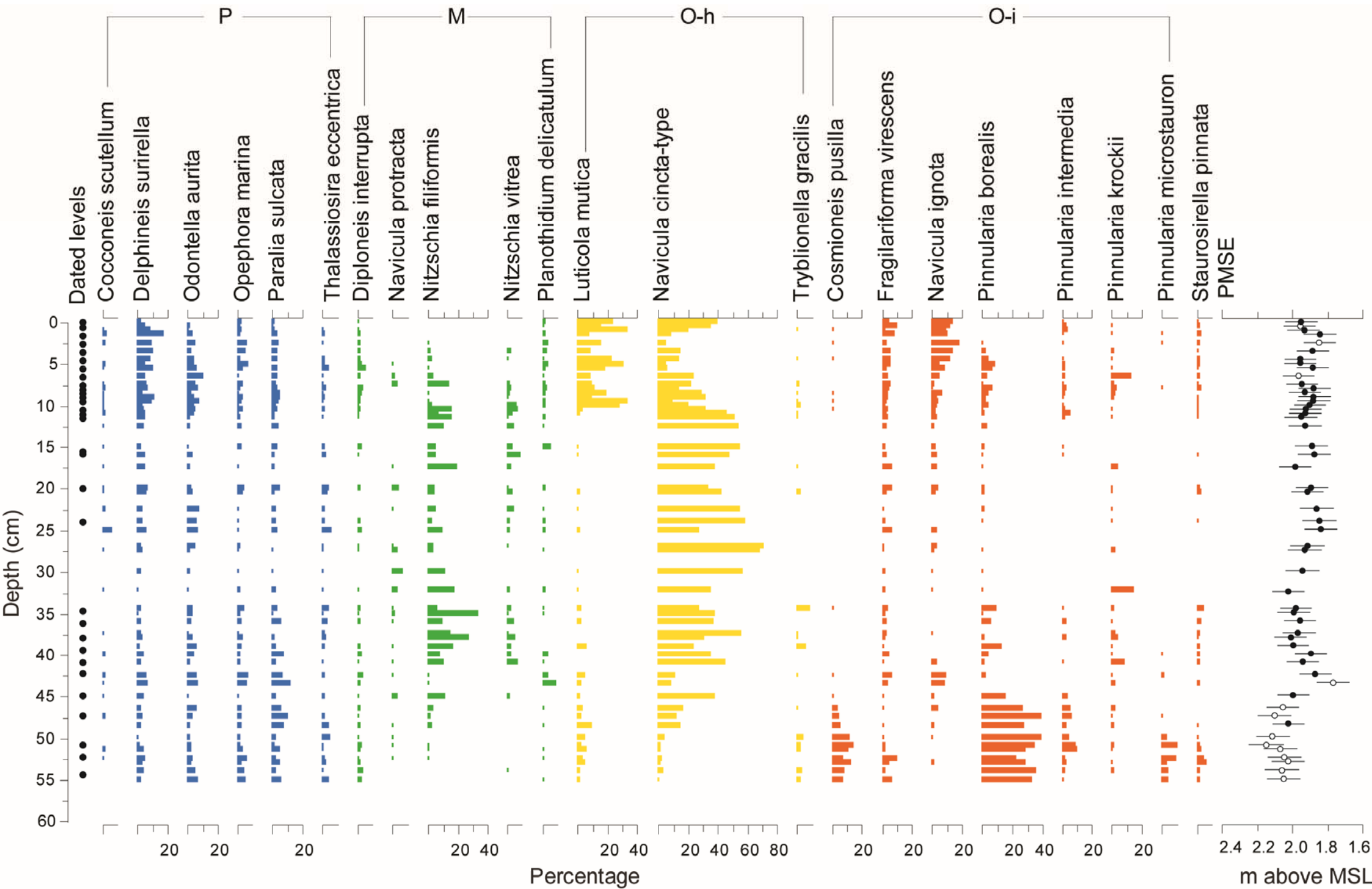
C

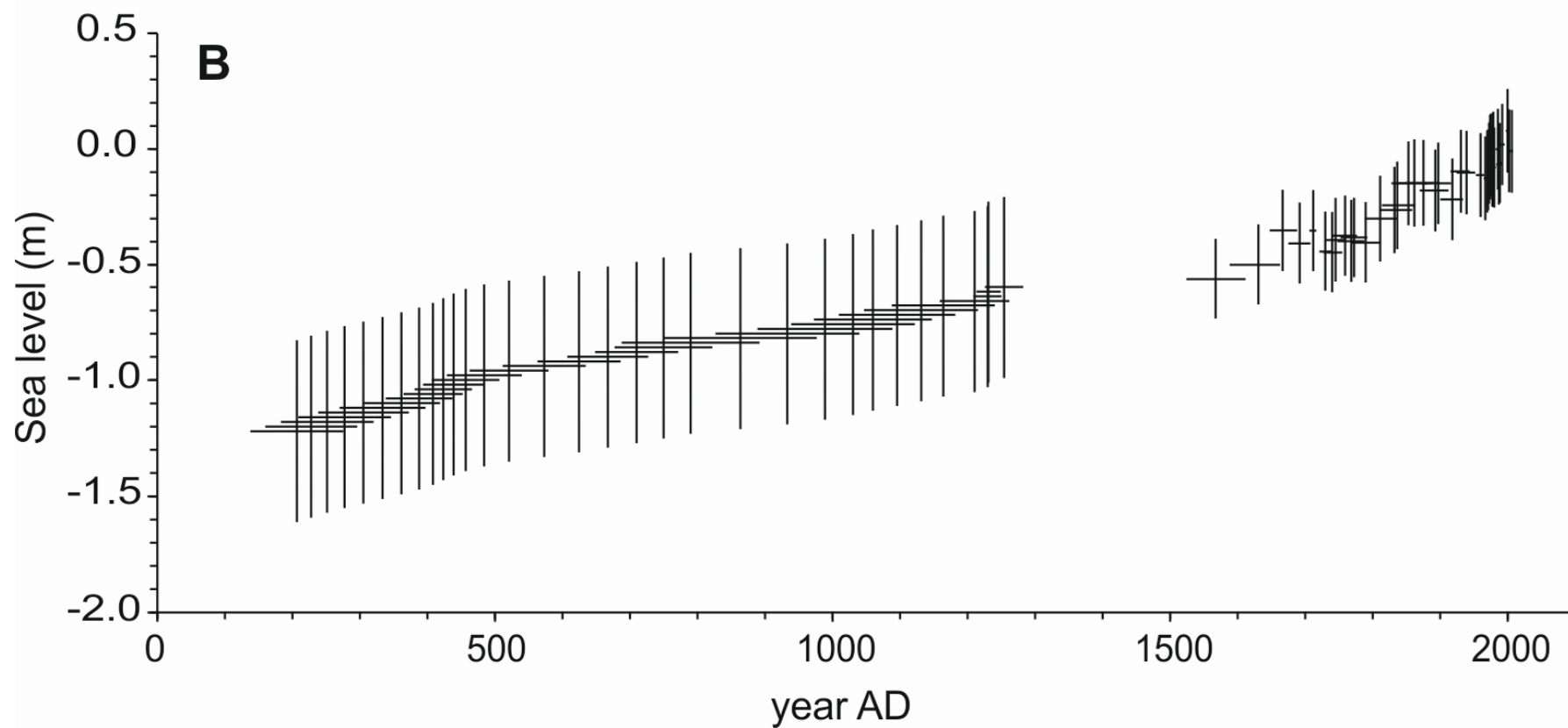
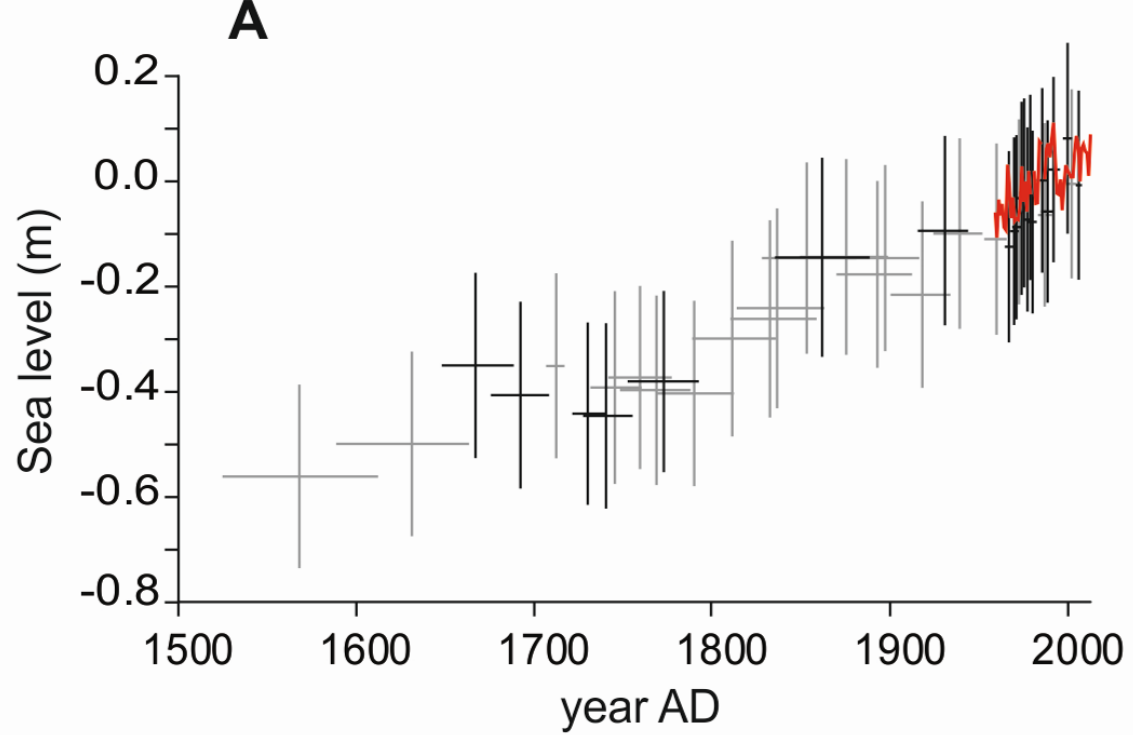


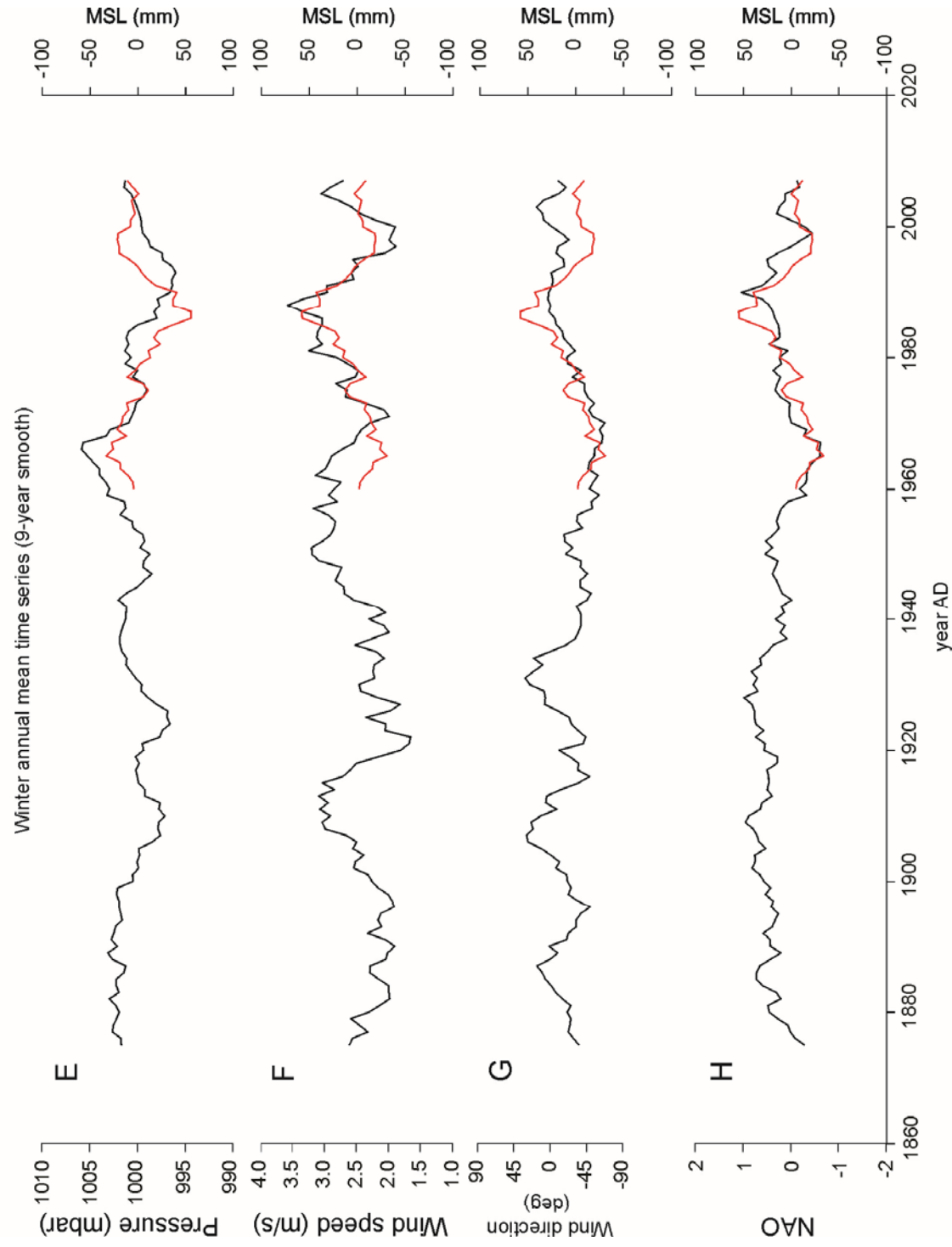
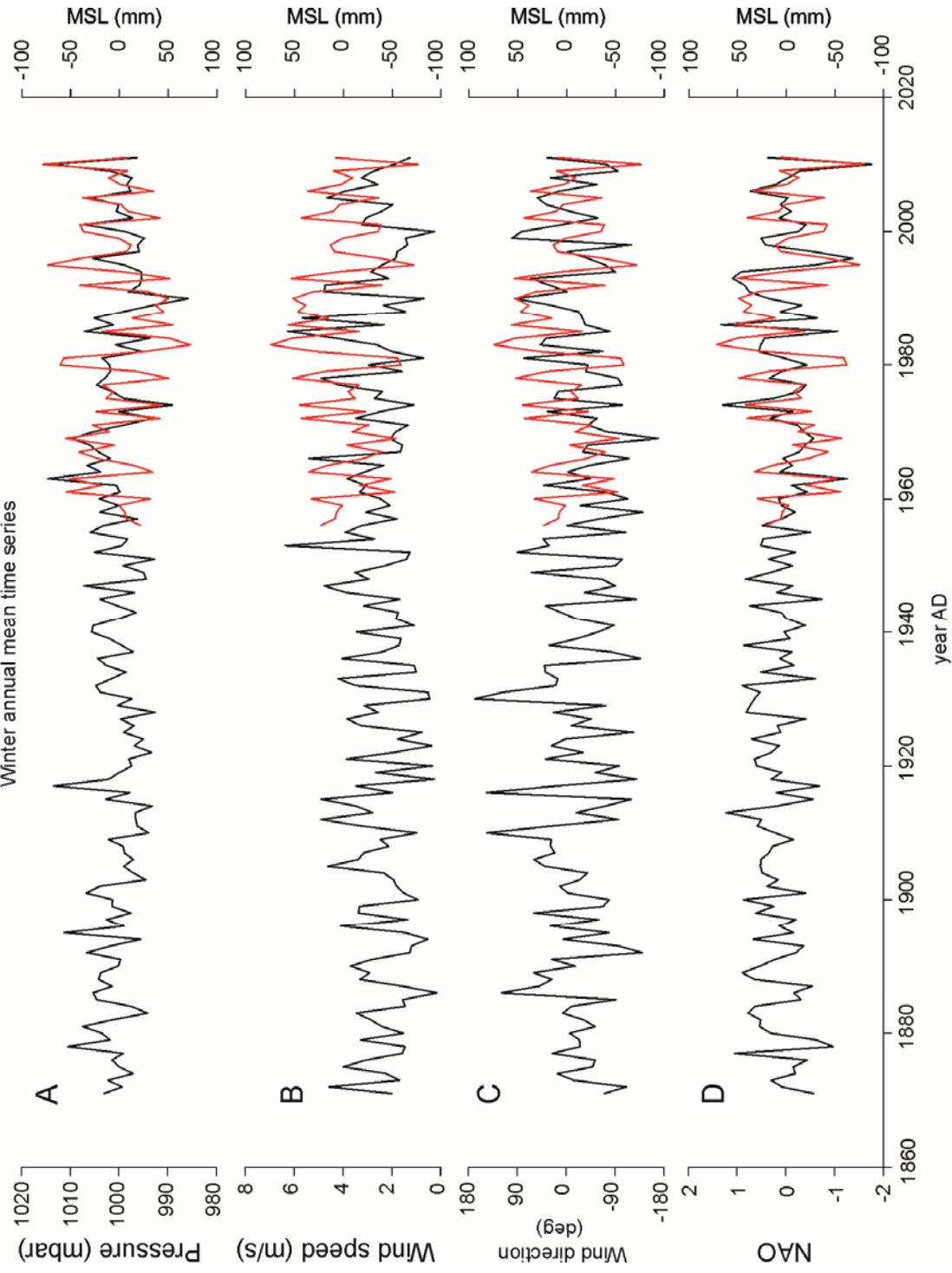


A**B****C****D**

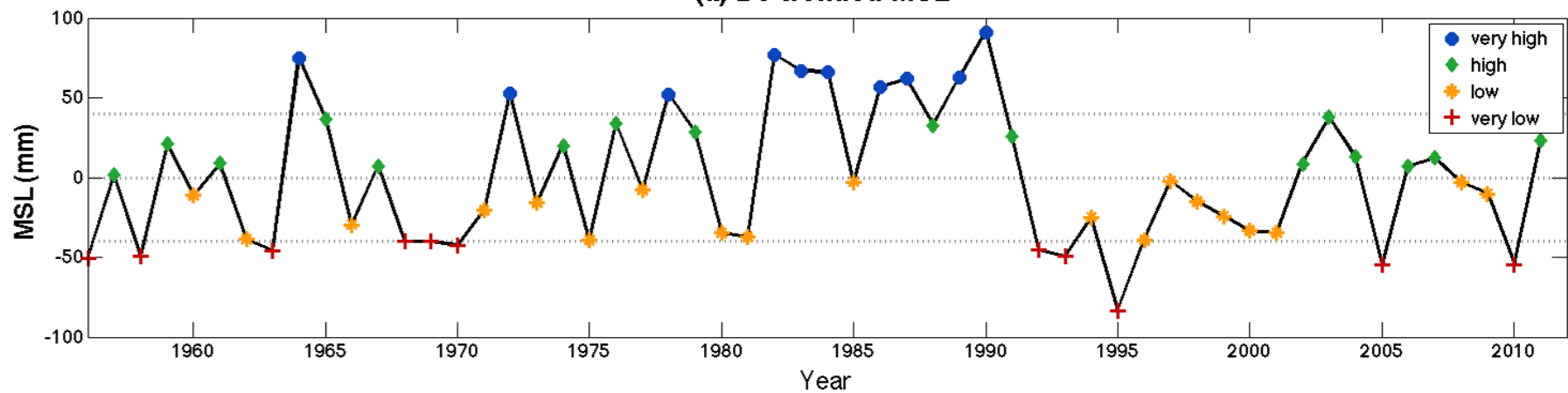




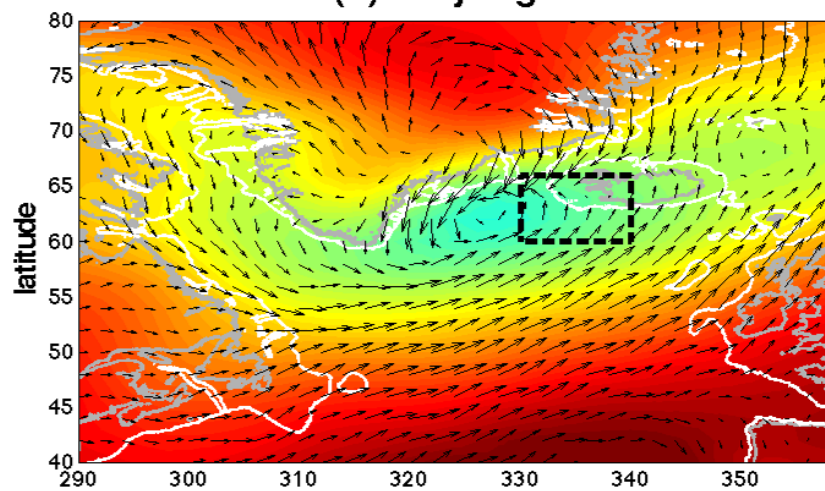




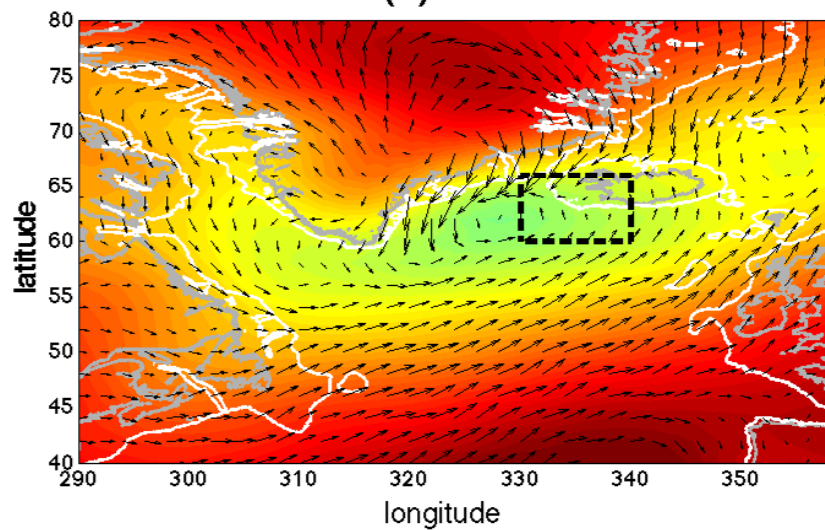
(a) De-trended MSL



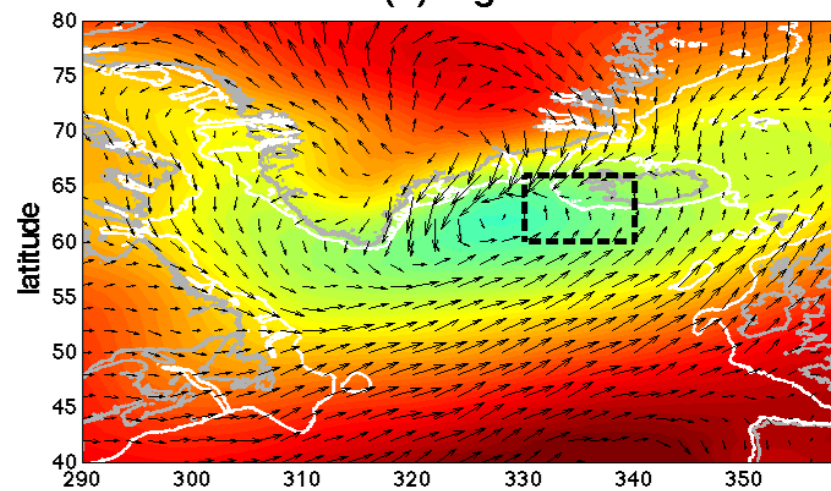
(b) Very High



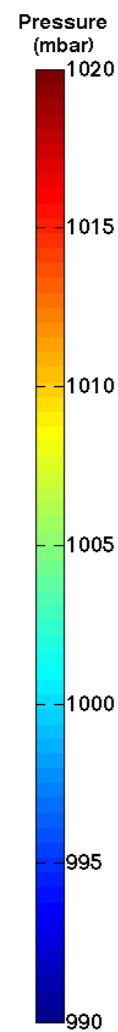
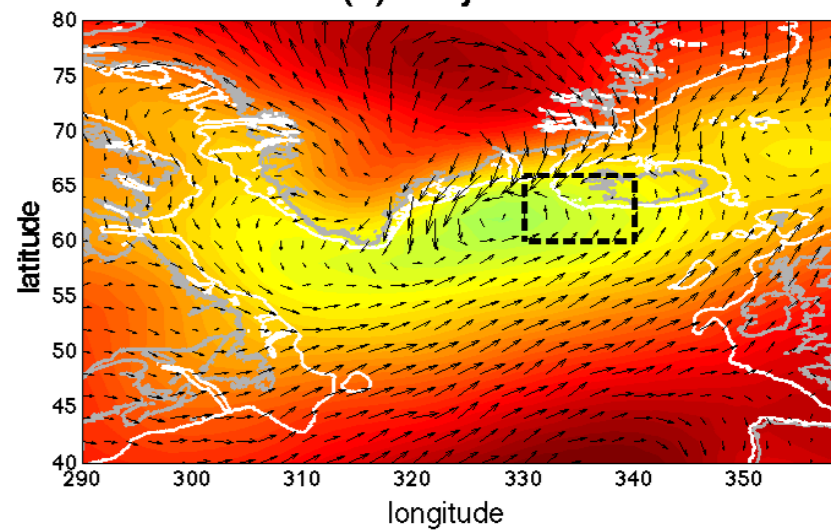
(d) Low

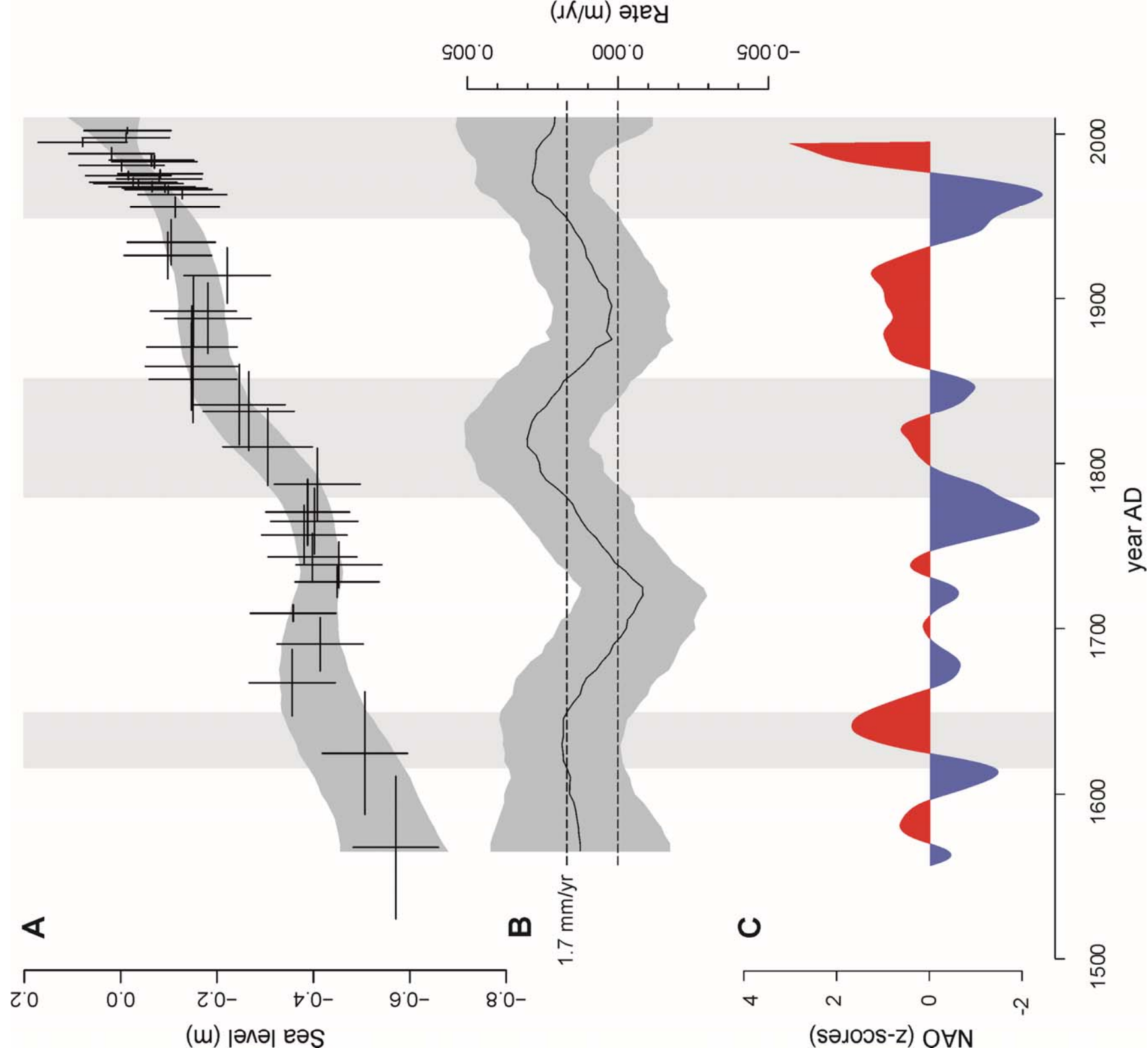


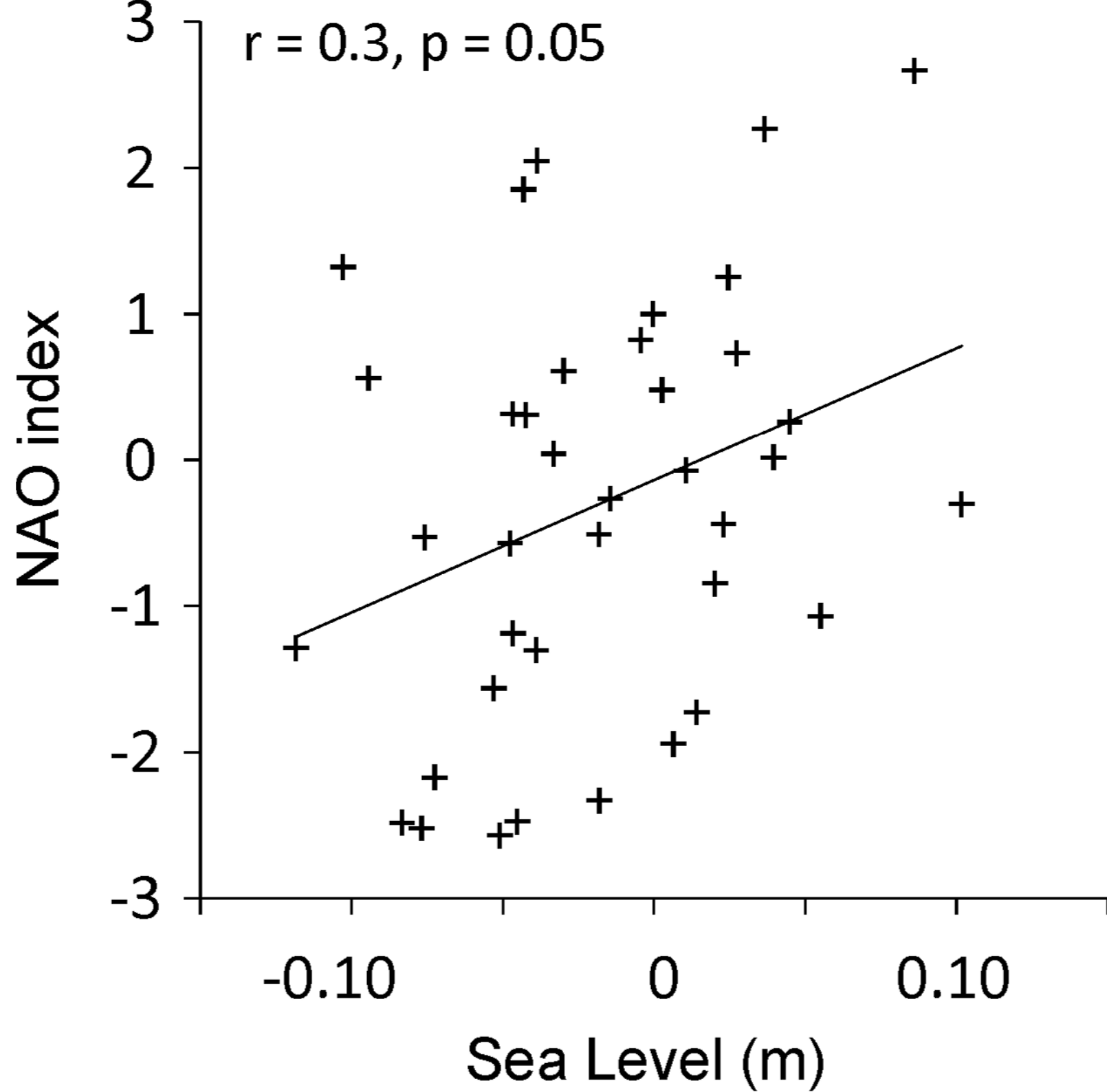
(c) High



(e) Very Low







Depth of date (cm)	Depth of modelled age (cm)	Source	Dating method/ marker	Lab. Code	Dry weight (mg)	Material	¹⁴ C enrichment (%modern ±1s)	¹⁴ C year BP ±1s	Age	Modelled age AD	Min. age AD	Max. age AD
0.0	0.0	2	surface						2001±1	2001.6	1999.9	2003.4
0.5	0.5	2	¹³⁷ Cs						2000±1	1999.7	1998	2001.3
1.5	1.5	2	¹³⁷ Cs						1995±2	1995.4	1992.8	1998
2.5	2.5	2	¹³⁷ Cs						1990±3	1991.2	1987.8	1994.5
3.5	3.5	2	¹³⁷ Cs						1986±4	1987.6	1984	1991.3
4.5	4.5	2	¹³⁷ Cs						1982±4	1984.2	1980.6	1988
5.5	5.5	2	¹³⁷ Cs						1978±5	1981.2	1977.6	1984.6
6.5	6.5	2	¹³⁷ Cs						1974±6	1978.4	1975.4	1981.5
7.5	7.5	2	¹³⁷ Cs						1970±6	1975.9	1973.2	1978.2
8.2	8.2	1	¹⁴ C bomb	SUERC-32116	1.2	weevil (<i>Otiorhynchus</i> sp.) exoskeleton	140.08±0.87			1974.6	1971.8	1976.9
8.5	8.5	2	¹³⁷ Cs ²⁰⁶ Pb/ ²⁰⁷ Pb,						1965±7	1973	1970.6	1974.7
9.0	9.0	2	Pb/Li						1960±5	1971.3	1968.2	1973.8
9.5	9.5	2	¹³⁷ Cs						1961±8	1969.8	1967.1	1972.2
10.5	10.5	2	¹³⁷ Cs						1957±9	1966.9	1964.5	1969.5
11.1	11.0	1	¹⁴ C bomb	SUERC-32119	1.7	Plant detritus	172.09±0.91			1965.5	1963.4	1968.2
11.5	11.5	2	¹³⁷ Cs						1953±9	1962.7	1960.4	1965.3
15.9	16.0	1	¹⁴ C bomb	SUERC-32002	7.7	Plant detritus	127.04±0.25			1927	1911.9	1940.1
16.0	16.0	2	²⁰⁶ Pb/ ²⁰⁷ Pb						1925±10	1927	1911.9	1940.1
20.3	20.0	1	¹⁴ C bomb	SUERC-32502	4.1	Plant detritus	103.22±0.21			1893.8	1871.3	1912.8
24.1	24.0	1	¹⁴ C	SUERC-32003	3.2	Plant detritus	99.66±0.19	27±16		1858.6	1832.3	1885.2
34.5	34.5	1	¹⁴ C	SUERC-32005	6.4	Plant detritus	97.55±0.19	199±16		1770.5	1750.3	1790

36.0	36.0	2	¹⁴ C	AAR-8031	12.5	Plant detritus	n/a	105±47	1757.1	1739.4	1774.8
38.2	38.0	1	¹⁴ C	SUERC-32011	5.3	Plant detritus	97.79±0.19	180±16	1738.3	1725.4	1753.1
39.0	39.0	1	Katla 1721 ash					1721±1	1728.1	1719.4	1738
39.0	39.0	2	¹⁴ C	AAR-8032	6.2	Plant detritus	n/a	168±43	1728.1	1719.4	1738
39.0	39.0	2	declination					1820±20	1728.1	1719.4	1738
41.0	41.0	1	¹⁴ C	SUERC-32012	7.1	Plant detritus	97.59±0.20	196±16	1690.6	1674	1706.5
42.2	42.5	1	¹⁴ C	SUERC-39555	3.1	Plant detritus	97.84±0.43	175±35	1665.5	1646.7	1686.9
44.9	45.0	1	¹⁴ C	SUERC-40502	2	Plant detritus	98.16±0.48	149±39	1630.1	1587.9	1661.9
47.2	47.5	1	¹⁴ C	SUERC-39565	4.1	Weevil	96.37±0.42	297±35	1585.8	1542.2	1628.3
51.0	51.0	2	¹⁴ C	AAR-8033	8.4	Plant detritus	n/a	314±36	1523.1	1483.1	1567.3
52.3	52.5	1	¹⁴ C	SUERC-32503	4.2	Plant detritus	96.16±0.20	315±17	1495	1459.8	1534.6
54.1	54.0	1	¹⁴ C	SUERC-39556	2.8	Plant detritus	95.06±0.41	407±35	1460.9	1425.7	1501.6

Depth below surface (cm)	Height (m MSL)	Age AD	Age error (+2 σ)	Age error (- 2 σ)	I.M. (m MSL)	RSL (m)	RSL error (m, 2 σ)
0.0	1.940	2002	1.8	1.7	1.952	-0.012	0.181
1.0	1.930	1998	2.6	3.1	1.940	-0.010	0.181
1.5	1.925	1995	2.6	2.6	1.847	0.078	0.183
3.5	1.905	1988	3.7	3.6	1.887	0.018	0.178
4.5	1.895	1984	3.8	3.6	1.958	-0.063	0.175
5.0	1.890	1983	4.0	3.8	1.959	-0.069	0.176
5.5	1.885	1981	3.4	3.6	1.888	-0.003	0.177
7.5	1.865	1976	2.3	2.7	1.948	-0.083	0.175
8.0	1.860	1975	2.3	2.8	1.877	-0.017	0.177
8.5	1.855	1973	1.7	2.4	1.933	-0.078	0.176
9.0	1.850	1971	2.5	3.1	1.877	-0.027	0.181
9.5	1.845	1970	2.4	2.7	1.882	-0.037	0.185
10.0	1.840	1968	3.1	3.1	1.903	-0.063	0.177
10.5	1.835	1967	2.6	2.4	1.928	-0.093	0.176
11.0	1.830	1966	2.7	2.1	1.930	-0.100	0.180
11.5	1.825	1963	2.6	2.3	1.955	-0.130	0.183
12.5	1.815	1956	5.7	6.9	1.931	-0.116	0.183
15.0	1.790	1935	12.7	14.7	1.895	-0.105	0.182
16.0	1.780	1927	13.1	15.1	1.879	-0.099	0.182
17.5	1.765	1915	15.7	17.8	1.987	-0.222	0.178
20.0	1.740	1894	19.0	22.5	1.892	-0.152	0.178
20.5	1.735	1890	19.3	23	1.918	-0.183	0.179
22.5	1.715	1872	23.5	25.8	1.865	-0.150	0.187
24.0	1.700	1859	26.6	26.3	1.850	-0.150	0.191
25.0	1.690	1850	27.7	25.1	1.842	-0.152	0.183
27.0	1.670	1834	26.3	22.6	1.918	-0.248	0.191
27.5	1.665	1830	25.9	22.1	1.933	-0.268	0.189
30.0	1.640	1809	24.6	22.3	1.946	-0.306	0.188
32.5	1.615	1787	22.2	21.3	2.026	-0.411	0.177
34.5	1.595	1771	19.5	20.2	1.983	-0.388	0.174
35.0	1.590	1766	19.1	20.4	1.995	-0.405	0.181
36.0	1.580	1757	17.7	17.7	1.960	-0.380	0.176
37.5	1.565	1743	15.0	13.6	1.964	-0.399	0.185
38.0	1.560	1738	14.8	12.9	2.014	-0.454	0.178
39.0	1.550	1728	9.9	8.7	1.999	-0.449	0.175
40.0	1.540	1710	4.8	5.6	1.898	-0.358	0.177
41.0	1.530	1691	15.9	16.6	1.944	-0.414	0.179
42.5	1.515	1666	21.4	18.8	1.872	-0.357	0.177
45.0	1.490	1630	31.8	42.2	1.997	-0.507	0.177
48.5	1.455	1567	43.9	42.8	2.025	-0.570	0.176